Power System Stability with High Shares of Grid-forming and Grid-following Inverters

I / II – Fundamentals and Advanced Topics

Dr. Sijia Geng, Assistant Professor

Department of Electrical and Computer Engineering

JOHNS HOPKINS UNIVERSITY

DTU PES Summer School
Technical University of Denmark (DTU), Copenhagen, Denmark, May 19, 2026

Outline

Lecture 1 - Fundamentals

- Background of power systems with high shares of inverter-based resources
- Modeling and dynamical responses of GFM and GFL inverters
- Fundamental stability concepts
- (Structural instability)

Lecture 2 – Advanced Topics

- Scale-free decentralized stability and next-generation grid codes
- Safety-critical GFM control with assignable voltage behavior and current limiting
- Singular solution space boundary via differential geometry

Background

Power systems with high share of power electronic devices

Inverter-Based Resources

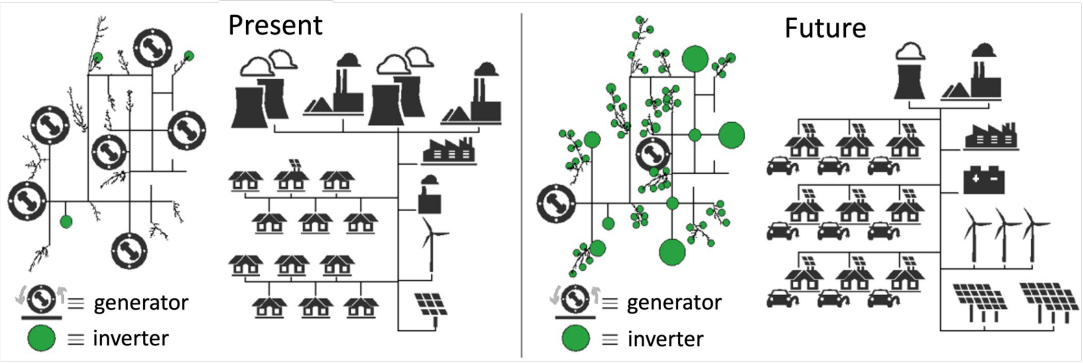

What's changing

Synchronous generators (rotating mass, slow) → power electronics (fast, software-controlled).

What this costs us

Natural voltage source behavior, fault currents, and inertia of physical machines — all lost unless we put them back via control.

- Electrical generator
  - Synchronous machines: Rotor spins at synchronous speed.

Source: Y. Lin et al., "Research roadmap on grid-forming inverters," Nat. Renew. Energy Lab., Golden, CO, USA, Tech. Rep. NREL/TP-5D00-73476, Nov. 2020.

Inverter-Based Resources

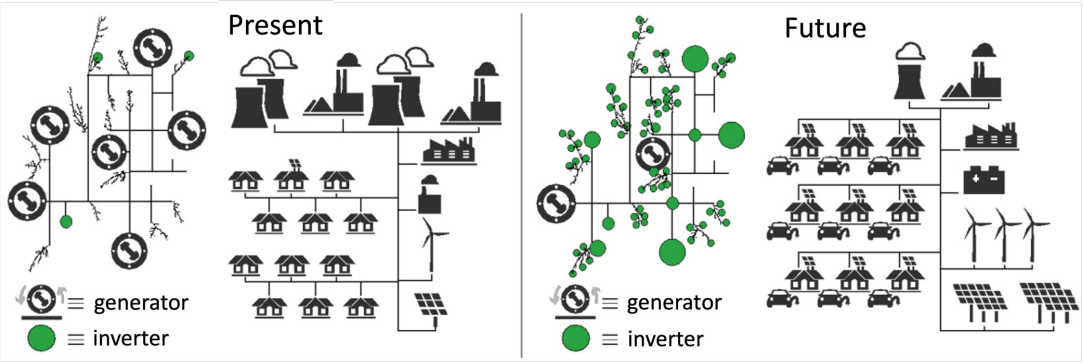

What's changing

Synchronous generators (rotating mass, slow) → power electronics (fast, software-controlled).

What this costs us

Natural voltage source behavior, fault currents, and inertia of physical machines — all lost unless we put them back via control.

- Electrical generator
  - Synchronous machines: Rotor spins at synchronous speed.
  - Inverter-based resources: The dynamic behavior (as seen from the grid) is dominated by control loops, not the physics of the machines. PE-based characteristics and limits.

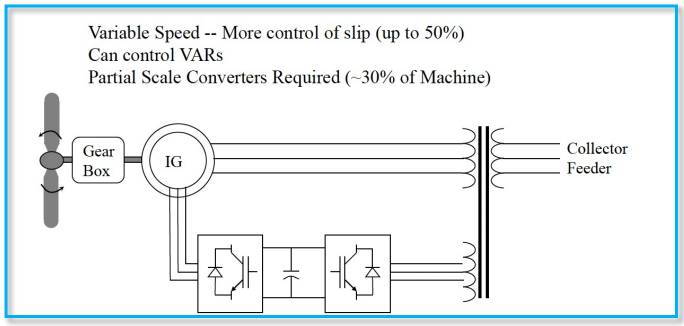

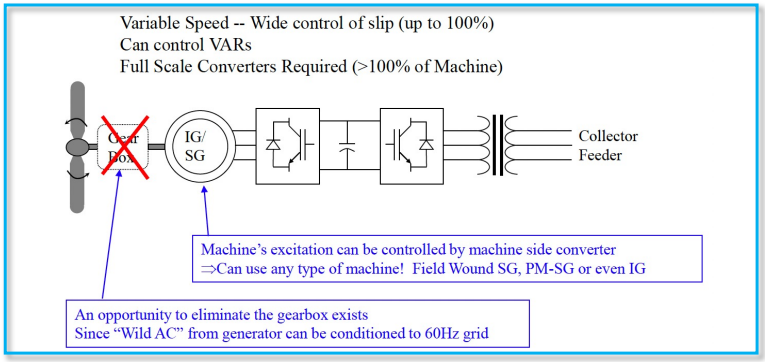

Various Control Strategies for IBRs

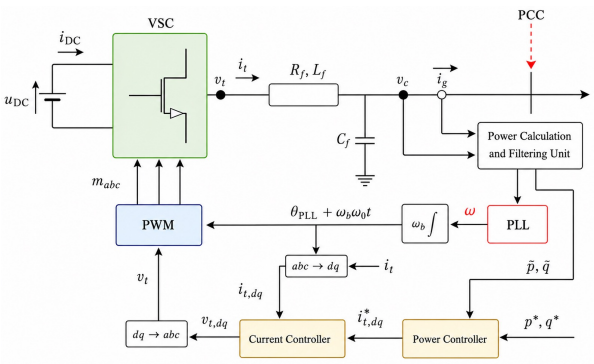

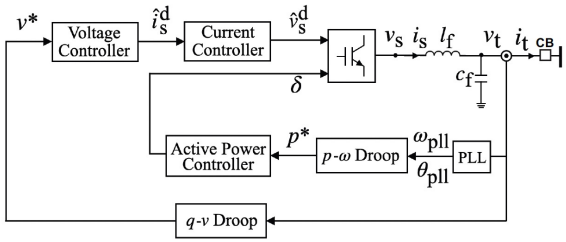

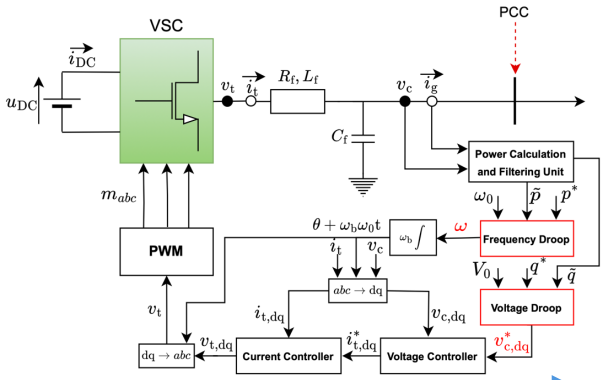

Grid-following[1]

- Current source: Injects active & reactive power to the grid.
- "Follow": Frequency is set to be synchronized with the existing grid voltage waveform using PLL.
- Drawbacks: Poorly damped oscillations in weak network.

Unified grid-forming/following[2]

- Unified GFM/GFL control: Incorporates both PLL and droop.
- Regulate voltage magnitude and active power.

Grid-forming[3]

- Voltage source: Set voltage magnitude and angle.
- "Forming": Frequency is set by droop function of exported power or VSM.
- Advantages: Black-start capability; Support weak network.

[1] Sushobhan Chatterjee and Sijia Geng. "Voltage Stability of Inverter-Based Systems: Impact of Parameters and Irrelevance of Line Dynamics." IEEE PowerTech, 2025.
[2] Sijia Geng, and Ian A. Hiskens. "Unified grid-forming/ following inverter control." IEEE Open Access Journal of Power and Energy, 2022.
[3] Sushobhan Chatterjee and Sijia Geng. "Effects of Line Dynamics on the Stability Margin to Hopf Bifurcation in Grid-Forming Inverters." IREP 2025 and Sustainable Energy, Grids and Networks (SEGAN), 2025.

Challenges in IBR-Dominated Power Systems

- New forms of dynamics and instability (v.s. swing equation)
  - Control-dominated nature: Droop[1], VSM[2], VOC[3], Unified[4], PLL-based GFL[5], etc.
  - Loss of time-scale separation: IBR operating times in milliseconds, which may interact with filter & line dynamics.
  - Operational limits and characteristics due to power electronics.
- Outdated tools for stability assessment, control, operation, planning:
  - Highly variable generation/load, and hence, operating points.
  - Increased system complexity and nonlinearity.
  - Model uncertainty (OEM-specific proprietary models) and heterogeneity.

[1] M. Chandorkar, et. Al, "Control of parallel connected inverters in standalone ac supply systems," IEEE TIA, 1993
[2] Beck, Hesse, "Virtual synchronous machine," Electrical Power Quality & Utilisation, 2007
[3] Johnson, Dhople, Hamadeh, Krein, "Synchronization of nonlinear oscillators in an LTI electrical power network," TCAS-I, 2014
[4] Sijia Geng, and Ian A. Hiskens. "Unified grid-forming/ following inverter control." IEEE Open Access Journal of Power and Energy, 2022.
[5] Sushobhan Chatterjee and Sijia Geng. "Voltage Stability of Inverter-Based Systems: Impact of Parameters and Irrelevance of Line Dynamics." IEEE PowerTech, 2025.

Sub-Synchronous Oscillations (SSO)

- SSO of 16-19 Hz observed by AEMO on various occasions from 2020-2021 in the West Murray Zone.

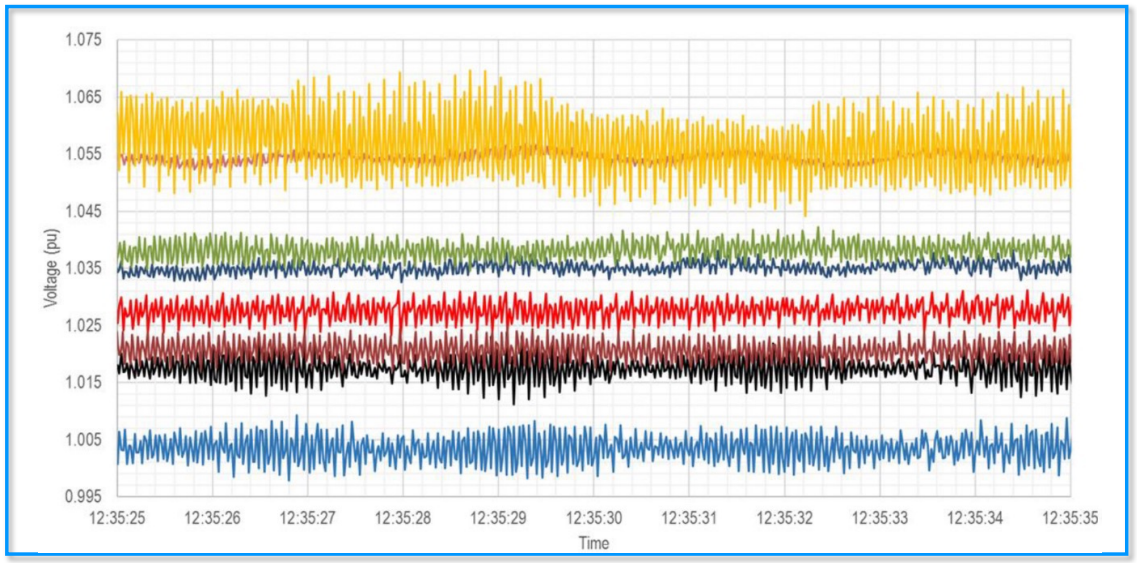

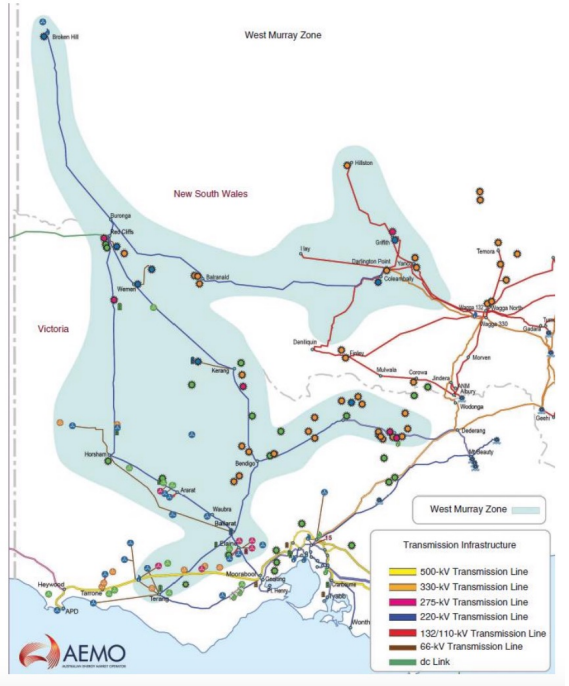

Source: National Electricity Market, "West Murray Zone Power System Oscillations 2020-2021", February 2023.

Effects of Power Electronic Loads

- Power electronic loads behave like constant power.
  - e.g., EVs, energy-efficient lighting.
  - Constant admittance: $P_d = K_a V_d^2$
  - Constant power: $P_d = K_p$
  - Loss of structural stability (bifurcation).

- Additional challenge for grid stability.
  - Shut down below a certain voltage.
  - Fast transition from full power to zero.

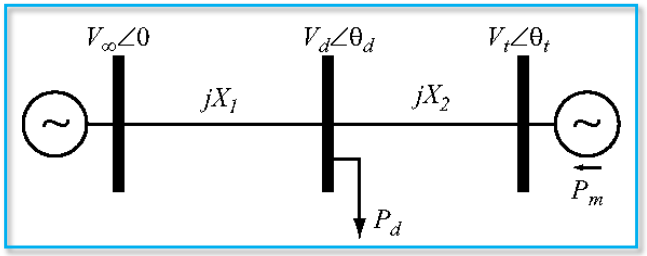

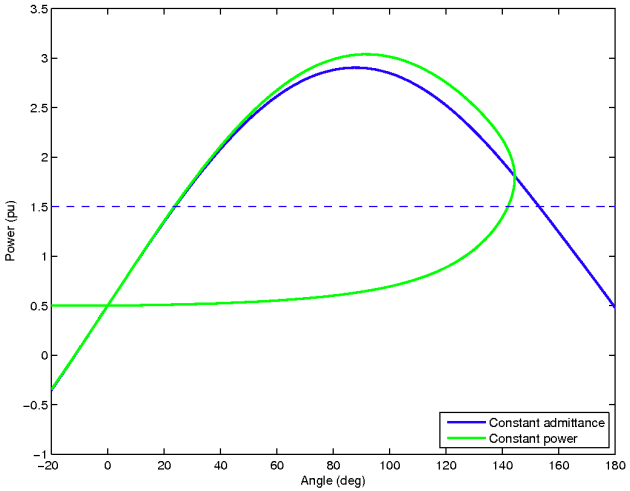

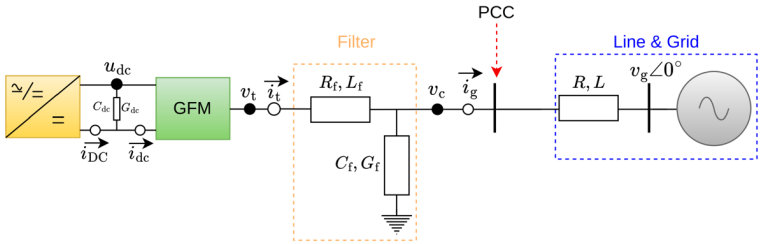

Modeling and Dynamics of Inverter-Based Resources

- Grid codes for GFM, GFL, etc
- Current limiting and hybrid dynamics
- Transmission line dynamics

Generic Control Structure of IBRs

- IBR architecture can generally be represented using a generic schematic (dq-frame).
  - Grid interacting functions: PLL (for GFL), droop/VSM (for GFM), etc.
  - Outer-loop controller: Power/DC-side voltage (for GFL), DC-side/AC-side voltage (for GFM), etc.
  - Inner-loop controller: Usually current.

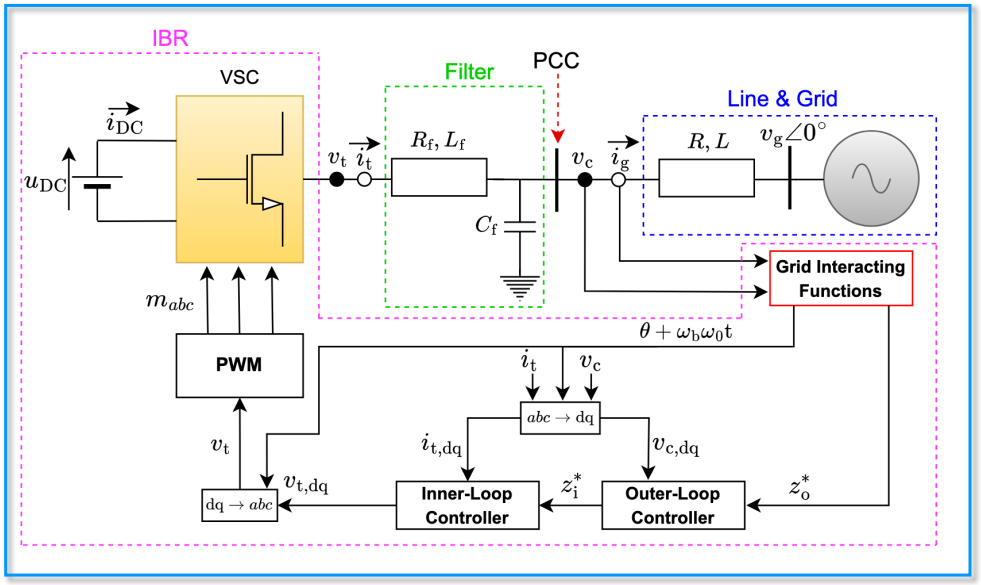

Typical Response time of IBR controllers

Controller	Response time
Inner current	1 ms – 5 ms
Voltage	10 ms – 100 ms
Power	100 ms – 500 ms
PLL	500 ms

Source: Sushobhan Chatterjee and Sijia Geng, "Voltage Stability of Inverter-Based Systems: Impact of Parameters and Irrelevance of Line Dynamics." IEEE PowerTech, 2025.

Grid Codes for GFM and GFL Inverters

- GFM definition by NERC[1]:

  "GFM IBR controls maintain an internal ***voltage*** **phasor**, i.e., AC voltage magnitude and angle, that is **constant or nearly constant** in the **sub-transient to transient time frame**."

- UNIFI Specifications[2]: Time-dependent control objectives of GFL/GFM inverter:

	Within 5 cycles (83 ms)	Within tens of cycles	Beyond 1-2 seconds
Legacy GFL	Maintain output current unchanged	Maintain output PQ per (transient) setpoints	MPPT, f and/or V regulation per commands
GFM	Maintain desired voltage phasor	Adjust V and f to sync with other sources (GFM/SG)	

	Within 50 ms		Beyond 50 ms
New GFL	Maintain output current unchanged	Maintain output PQ per (transient) setpoints	MPPT, f and/or V regulation per commands

[1] NERC, "Grid forming technology: Bulk power system reliability considerations," tech. rep., North American Electric Reliability Corporation (NERC), Atlanta, GA, USA, 2021.
[2] UNIFI Consortium, UNIFI Specifications for Grid-forming Inverter-based Resources, Version 3 (draft), 2025.

Grid Codes for GFM and GFL Inverters

- NERC defines three core functional performance tests for GFM BESS in terms of observable response (frequency, voltage, phase/angle) with pass/fail success criteria.
  - Trip of last synchronous machine → System must remain stable with only BESS in GFM role.
  - Large disturbance ride-through → BESS must hold grid within bounds through faults/transients.
  - V/f support under stress → BESS must follow specified droop characteristics and stabilize.
- Applies to charging/discharging transitions & max-power operation cases.
- Focus: System-level stability behavior; not a prescriptive numeric grid code.

Source: NERC White Paper: Grid Forming Functional Specifications for BPS-Connected Battery Energy Storage Systems, 2023

Comparison of Selected GFM Specifications

Org/Region	RoCoF / Frequency	Angle/Phase Step	System Strength / Faults	Other Notes
ERCOT (NA)	RoCoF 1 Hz/s profile; H ≥ 2.5 s; droop ≤ 5%	±10°, ±25°; ≥0.2 pu ΔP; ≤1 cycle to 90%	Stable down to SCR 1.2 with 4-cycle faults	Small V steps ±3% → ≥0.03 pu ΔQ; ≤1 cycle
NERC (NA)	Functional tests; settle per droop & deadband	Trip-of-last-SG scenarios (stability focus)	Model quality emphasis	-
NGESO (EU)	+1 / −2 Hz/s ramps within 47–52 Hz	Large phase-jump survivability (~60°)	Control BW guideline ~5 Hz	Best-practice verification set
Fingrid (EU)	RoCoF trip only if > 4 Hz/s for ≥250 ms	Ride-through permanent ±30° vector shift	Coordination of fast GFM + slow controls	Discourages RoCoF/vector-shift protection
AEMO (AU)	RoCoF up/down tests (up to ~4 Hz/s)	±10/±30/±60°; ≥0.2 pu ΔP; 90% ≤ 15–25 ms	SCR step-down to ~1.25 with faults	Voltage restoration < 0.1 s (bounds)
India (AS)	Frequency response per CEA/CERC	(no explicit angle step in code)	LVRT/HVRT required	PF 0.95 lag ↔ 0.95 lead dynamic VAR
China (AS)	Primary freq control + inertia response	(test details in GB/T 36548-2024)	Fault ride-through specified	Power quality + model/test requirements

PLL-Based GFL IBR

- 9th order model
  - Grid-interacting functions: PLL (2nd order)
  - Inner control loops: DC-link; active and reactive power controllers

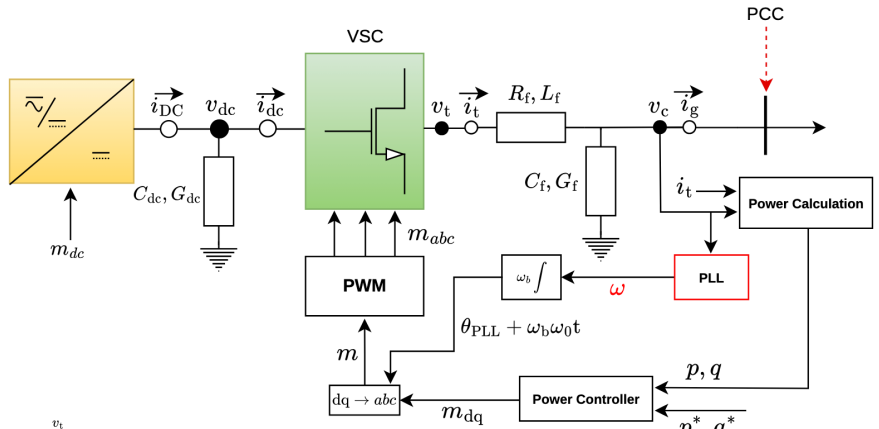

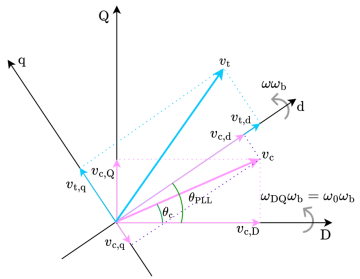

Differential Equations:

$$\dot{\theta}_{PLL} = \omega_b \delta\omega_{PLL}$$

$$\dot{\gamma_{PLL}} = -K_\gamma \gamma_{PLL} + K_v v_{c,q}$$

$$\dot{v_{dc}} = -\frac{G_{dc}}{C_{dc}} v_{dc} + \frac{1}{C_{dc}} (i_{DC} - i_{dc})$$

$$\dot{\boldsymbol{i}}_t = \frac{\omega_b}{L_f} (\boldsymbol{v}_t - \boldsymbol{v}_c) - \frac{R_f}{L_f} \omega_b \boldsymbol{i}_t + \omega\omega_b \begin{bmatrix} 0 & 1 \\ -1 & 0 \end{bmatrix} \boldsymbol{i}_t$$

$$\dot{\boldsymbol{v}}_c = \frac{\omega_b}{C_f} (\boldsymbol{i}_t - \boldsymbol{i}_g) - \frac{G_f}{C_f} \omega_b \boldsymbol{v}_c + \omega\omega_b \begin{bmatrix} 0 & 1 \\ -1 & 0 \end{bmatrix} \boldsymbol{v}_c$$

$$\dot{\boldsymbol{m}} = -K_m \boldsymbol{m} + K_{PC} \begin{bmatrix} p^* - p \\ q^* - q \end{bmatrix}$$

Algebraic Equations:

$$\omega - \omega_0 - \delta\omega_{PLL} = 0$$

$$\delta\omega_{PLL} - K^P_{PLL} v_{c,q} - K^I_{PLL} \gamma_{PLL} = 0$$

$$i_{DC} - i^0_{dc} - K^P_{DVC} (v^*_{dc} - v_{dc}) = 0$$

$$i_{dc} - b\boldsymbol{m}^T \boldsymbol{i}_t = 0$$

$$\boldsymbol{v}_t - b\boldsymbol{m} v_{dc} = 0$$

$$p - v_{c,d} i_{t,d} - v_{c,q} i_{t,q} = 0$$

$$q - v_{c,q} i_{t,d} + v_{c,d} i_{t,q} = 0$$

Droop-Based GFM Model

- 11th (Ideal DC side) and 13th (DC-link)-order model
  - Grid-interacting functions: Frequency droop and voltage droop
  - Inner control loops: DC-link and dq-axis voltage and current controllers

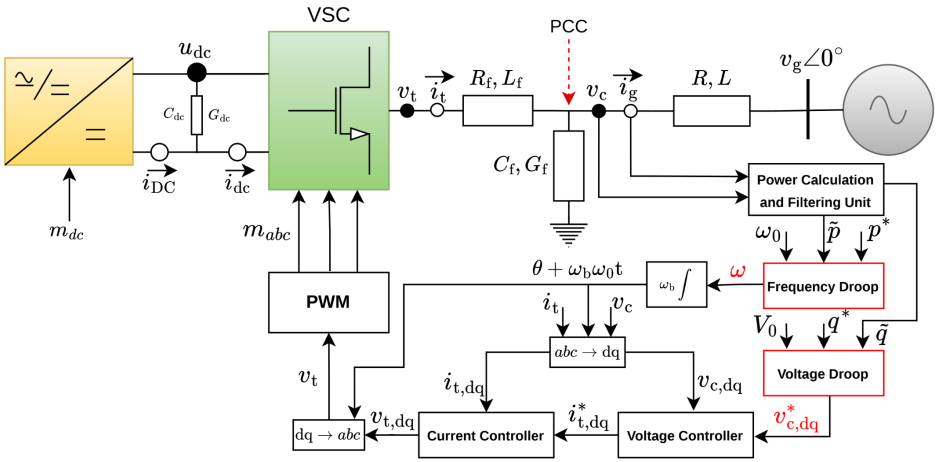

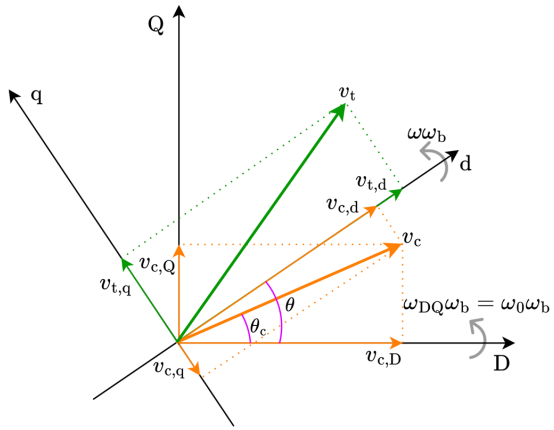

VSM-Based GFM Model

- 12th (Ideal DC side) and 14th (DC link)-order model
  - Grid-interacting functions: VSM and voltage droop
  - Inner control loops: DC-link and dq-axis voltage and current controllers

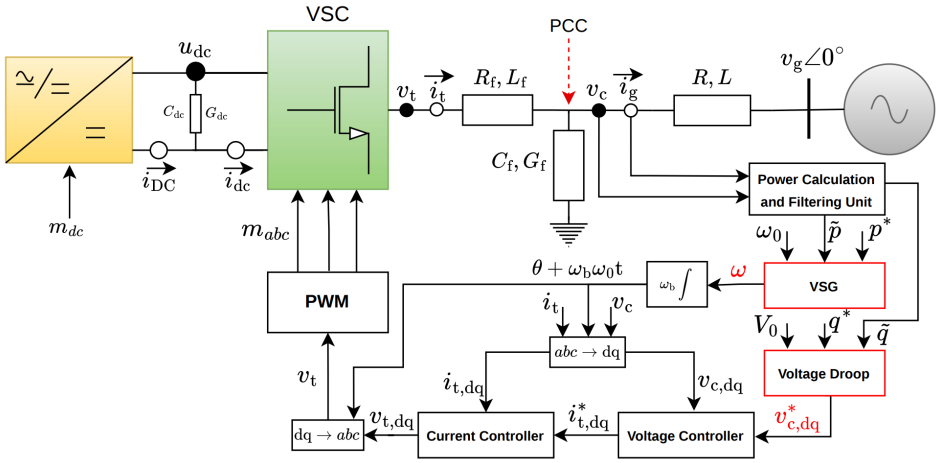

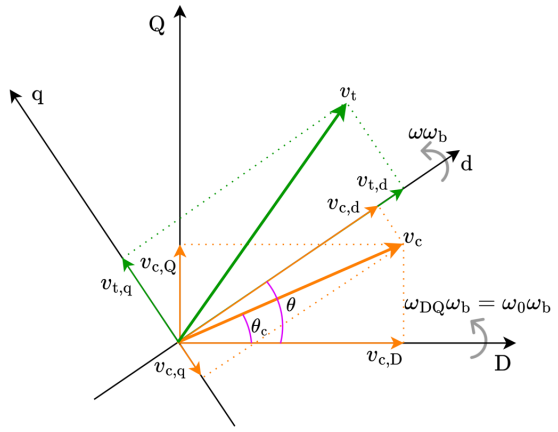

Current Limiters in IBRs

- Reference Modification limiters[1]

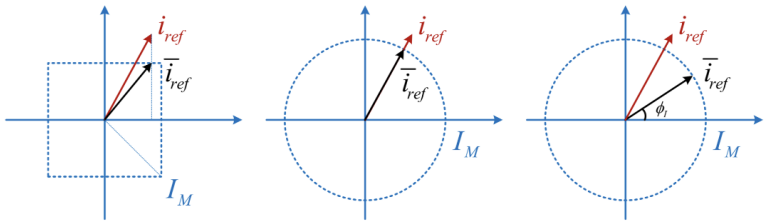

Figure: (i) Instantaneous; (ii) Magnitude; (iii) Priority-based.

PQ Priority Current Limiting Algorithm

Q Priority (PQFlag=0)	P Priority (PQFlag=1)
$I_{q\max\_GFL} = k_f I_{\max}$ $I_{q\min\_GFL} = -I_{q\max\_GFL}$ $I_{p\max\_GFL} = \begin{cases} \sqrt{I_{\max}^2 - I_{q\_GFL}^2}, I_{\max}^2 \geq I_{q\_GFL}^2 \\ 0, I_{\max}^2 < I_{q\_GFL}^2 \end{cases}$ $I_{p\min\_GFL} = -I_{p\max\_GFL}$	$I_{p\max\_GFL} = k_f I_{\max}$ $I_{p\min\_GFL} = -I_{p\max\_GFL}$ $I_{q\max\_GFL} = \begin{cases} \sqrt{I_{\max}^2 - I_{p\_GFL}^2}, I_{\max}^2 \geq I_{p\_GFL}^2 \\ 0, I_{\max}^2 < I_{p\_GFL}^2 \end{cases}$ $I_{q\min\_GFL} = -I_{q\max\_GFL}$

- Anti-windup (AW) control[2]

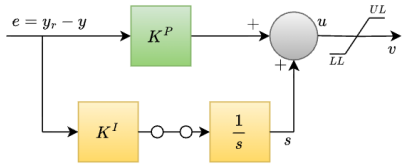

Figure: Regulator with AW based on tracking integration.

Limiters that could be present in IBRs:

- DC current magnitude → Instantaneous
- DC current rate limiter

- PWM modulation → Magnitude
- AW current controller → Tracking

- AC current magnitude → Q-Priority
- AW voltage controller → Tracking

[1] Fan et al., "A review of current-limiting control of grid-forming inverters under symmetrical disturbances", IEEE OJPE (2022).
[2] Bohn and Atherton, "An analysis package comparing PID anti-windup strategies," in IEEE Control Systems Magazine", IEEE CSM (1995).

Current Limiters in IBRs

- Hysteresis loops[1]

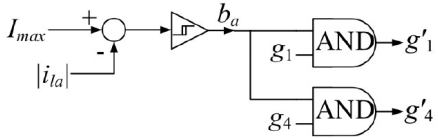

Figure: Hysteresis-based fault current limiter at PWM control layer.
Pros: Rapid response, seamless switchover between normal and fault modes. Cons: Requires quick fault-clearing protection devices, produces distorted current.

- Virtual impedance[2]

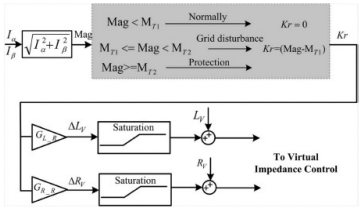

Figure: LVRT using adaptive impedance.
Pros: Less sensitive to harmonics and *hf* noises. Cons: Requires multi-conditional tracking and mode switchovers.

- Voltage limiters[3]

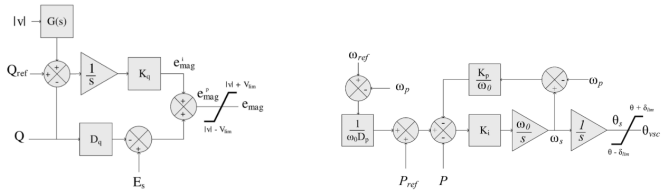

(a) Reactive power/voltage controller (b) Active power/frequency controller

Figure: Voltage limiting control strategy
Pros: Rapid switchover between island and grid modes during faults. Cons: Requires multi-conditional tracking and mode switchovers.

[1] Wei Du, et al. "A current limiting control strategy for single-loop droop-controlled grid-forming inverters under balanced and unbalanced faults." 2022 IEEE Energy Conversion Congress and Exposition (ECCE). IEEE, 2022. [2] Jinwei He and Yun Wei Li. "Analysis, design, and implementation of virtual impedance for power electronics interfaced distributed generation." IEEE Transactions on industry Applications 47.6 (2011): 2525-2538. [3] Jeffrey Bloemink and Iravani Reza. "Control of a multiple source microgrid with built-in islanding detection and current limiting." IEEE Transactions on Power Delivery 27.4 (2012): 2122-2132.

Hybrid Dynamics

- The anti-windup PI scheme, AC-side current limiter, and DC-side limiter introduce an important hybrid nature into the system dynamics.

Logic :-

$$
\begin{aligned}
&\text{if } (\text{UL Detector } \#1) < 0, && \text{Normal}\\
&(\text{UL Block } \#1) - 1 = 0\\
&(\text{UL Detector } \#1) - \gamma_d + I_{d,max} = 0\\
&\text{else}, && \text{UL triggerred}\\
&(\text{UL Block } \#1) = 0\\
&(\text{UL Detector } \#1) - i^*_{t,d} + i_{t,d} = 0\\
&\text{if } (\text{LL Detector } \#1) < 0, && \text{Normal}\\
&(\text{LL Block } \#1) - 1 = 0\\
&-(\text{LL Detector } \#1) - \gamma_d + I_{d,min} = 0\\
&\text{else}, && \text{LL triggered}\\
&(\text{LL Block } \#1) = 0\\
&-(\text{LL Detector } \#1) - i^*_{t,d} + i_{t,d} = 0
\end{aligned}
$$

$\Longrightarrow$

Pseudo-code :-

```
if ev(1) < 0
    ans(1) = y(1)-1;
    ans(2) = y(3)-x(1)+p(1);
else
    ans(1) = y(1);
    ans(2) = y(3)-y(6)+y(5);
end
if ev(2) < 0
    ans(3) = y(2)-1;
    ans(4) = -y(4)-x(1)+p(2);
else
    ans(3) = y(2);
    ans(4) = -y(4)-y(6)+y(5);
end
```

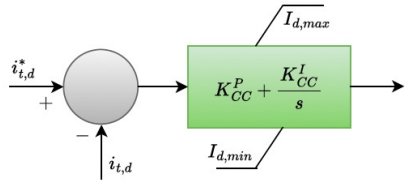

$\gamma_d \rightarrow$ integrator state.

ev $\rightarrow$ switching event, when upper or lower limit gets triggered.

Hybrid and Discrete Events

- Power system dynamics are typically described by a differential-algebraic equation (DAE) model:

$$\dot{x} = f(x, y), \qquad x(0) = x_0$$
$$0 = g(x, y)$$

- However, discrete events are ubiquitous in power systems. For example:
  - A transmission line trips (triggering event), voltages drop across the network, IBRs respond (consequent events).
  - An inverter meets its current limit. (System model changes.)
  - A circuit breaker opens due to faults in the main grid and a microgrid is formed (System (algebraic) states jump.)
  - A generator hits its reactive power limit and can no longer hold voltage constant. (System model changes.)

Capturing Hybrid and Discrete Events

- Accurate handling of switching events is vital to have any chance of replicating complex power system behavior.
  - Triggering event: Described by switching manifold.
  - System response: Switch of algebraic equations and/or state reset.
  - Away from event: Smooth DAE system.

- Differential-Algebraic Impulsive Switched (DAIS) model:

$$\dot{x} = f(x, y)$$

$$0_m = g(x, y) \triangleq \begin{cases} \underline{g}(x, y), & s(x, y) < 0 \\ \overline{g}(x, y), & s(x, y) > 0 \end{cases}$$

$$x^+ = h(x^-, y^-), \quad s(x, y) = 0$$

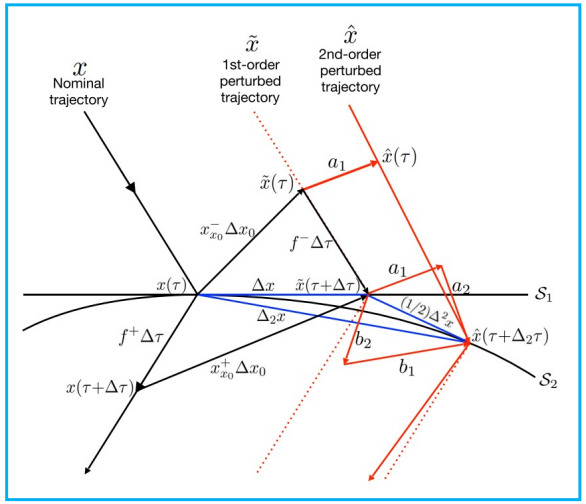

[1] Ian Hiskens and Jassim Alseddiqui, "Sensitivity, approximation, and uncertainty in power system dynamic simulation," IEEE Trans. Power Syst., vol. 21, no. 4, pp. 1808–1820, Nov. 2006

[2] Sijia Geng and Ian Hiskens. "Second-order trajectory sensitivity analysis of hybrid systems." IEEE Transactions on Circuits and Systems I: Regular Paper, 2019.

Example: Q-limit Induced Voltage Reduction

- Classic SMIB example assumes the generator will maintain a constant terminal voltage. However, in reality, the reactive power required to support the voltage is limited.
- Upon encountering this limit, the over-excitation limiter will act to reduce the terminal voltage.

$$\frac{d}{dt}\begin{bmatrix}\delta\\ \omega\end{bmatrix} = \begin{cases}\omega\\ \frac{1}{M}\left(P_m - \frac{V_\infty V_t}{X}\sin(\delta) - D\omega\right)\end{cases}$$

$$0 = \left(\frac{V_\infty V_t}{X}\sin(\delta)\right)^2 + \left(\frac{V_t^2}{X} - Q\right)^2 - \frac{V_\infty^2 V_t^2}{X^2}$$

$$0 = \begin{cases}V_t - V_{set}, & Q - Q_{max} < 0\\ Q - Q_{max}, & V_{set} - V_t > 0.\end{cases}$$

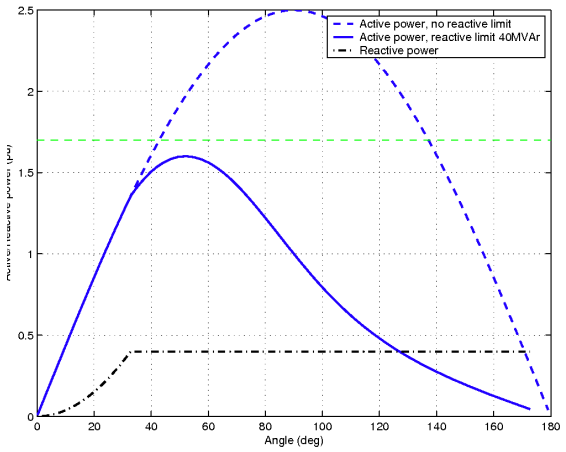

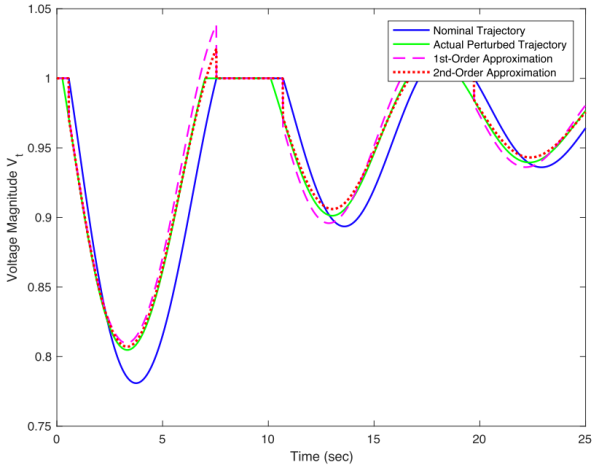

Source: Sijia Geng and Ian Hiskens. "Second-order trajectory sensitivity analysis of hybrid systems." IEEE Transactions on Circuits and Systems I: Regular Papers (2019).

Impacts of Transmission Line Dynamics?

- Conventional power system modeling ignores line dynamics; valid for slow synchronous machines but not necessarily for fast-acting IBRs operating on millisecond timescales[1,2].
- Instability risks increase when line dynamics are neglected, as shown in droop and unified inverters[3,4,5,6].

[1] Peponides et.al. "Singular perturbations and time scales in nonlinear models of power systems", *IEEE Transactions on Circuits and Systems, 1982.*
[2] Cheng et.al. "Real-world subsynchronous oscillation events in power grids with high penetrations of inverter-based resources", *IEEE Transactions on Power Systems, 2022.*
[3] Gross et.al. "The effect of transmission-line dynamics on grid-forming dispatchable virtual oscillator control", *IEEE Transactions on Control of Network Systems, 2019.*
[4] Geng et.al. "Unified grid-forming/following inverter control", *IEEE Open Access Journal of Power and Energy, 2022.*
[5] Vorobev et.al. "High-fidelity model order reduction for microgrids stability assessment", *IEEE Transactions on Power Systems, 2017.*
[6] Chatterjee et.al. "Sensitivity to Hopf Bifurcation in Grid-Following Inverters using normal vector methods", *Allerton Annual Conference, 2024.*

Static and Dynamic Line Models

- Dynamic line model: Captures electromagnetic transients using differential equations for network current flow, under global reference frame with speed ω_{DQ}.

$$\dot{i}_{\mathrm{g,D}} = \frac{\omega_{\mathrm{b}}}{L}\left(v_{\mathrm{c,D}} - v_{\mathrm{g,D}}\right) - \frac{R}{L}\omega_{\mathrm{b}} i_{\mathrm{g,D}} + \omega_{\mathrm{DQ}}\omega_{\mathrm{b}} i_{\mathrm{g,Q}},$$

$$\dot{i}_{\mathrm{g,Q}} = \frac{\omega_{\mathrm{b}}}{L}\left(v_{\mathrm{c,Q}} - v_{\mathrm{g,Q}}\right) - \frac{R}{L}\omega_{\mathrm{b}} i_{\mathrm{g,Q}} - \omega_{\mathrm{DQ}}\omega_{\mathrm{b}} i_{\mathrm{g,D}}.$$

- Static line model: At steady-state ($\omega_{DQ} = \omega_{ss}$), dynamic equations reduce to algebraic equations, typical of traditional power flow/impedance models.

$$i_{\mathrm{g,D}} = \frac{R}{Z^2}\left(v_{\mathrm{c,D}} - v_{\mathrm{g,D}}\right) + \frac{X}{Z^2}\left(v_{\mathrm{c,Q}} - v_{\mathrm{g,Q}}\right),$$

$$i_{\mathrm{g,Q}} = \frac{R}{Z^2}\left(v_{\mathrm{c,Q}} - v_{\mathrm{g,Q}}\right) - \frac{X}{Z^2}\left(v_{\mathrm{c,D}} - v_{\mathrm{g,D}}\right),$$

$$Z^2 = R^2 + X^2, \quad X = \omega_{\mathrm{DQ}} L.$$

Source: Sijia Geng and Ian Hiskens, "Unified grid-forming/following inverter control", *IEEE Open Access Journal of Power and Energy, 2022.*

Dynamic Response of Single-Inverter-Infinite-Bus Systems

- Droop-based and VSG-based GFM inverters connected to the grid
- No DC-link (Ideal DC side) and PI controlled DC-link modelling (Intermediate model)
- Anti-windup AC voltage controller + Q Priority-based AC current reference saturation limiter + DC-side current rate and instantaneous saturation limiter
- Fault scenarios: 3-phase fault at PCC

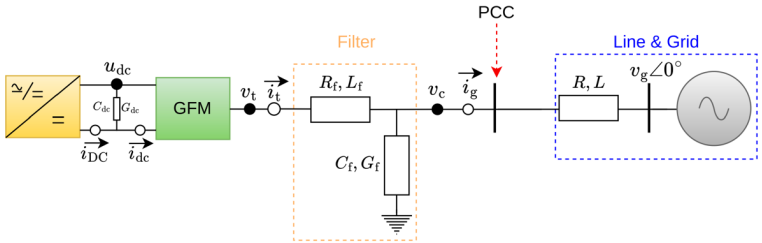

Observations

- Ideal and DC-link GFM models exhibit similar transient behavior without DC-limiters, but the behavior is more jittery under its presence.
- DC-link behavior exhibits higher incursions and slower recovery under the presence of DC-limiters, than without them.
- Dynamic lines exhibit more oscillatory behavior compared to static ones during fault recovery.
- Q-priority limiters can ensure fault ride-through (FRT) in almost all cases compared to P-priority, which causes the system to stagnate in saturation equilibriums.
- Presence of tracking-based Anti-Windup mechanism in voltage controllers ensure a stabilizing and faster FRT response.
- Fault ride-through with VSG is slightly slower than with droop control; however, it exhibits a better-damped response with reduced oscillations, as well as smaller frequency and DC-link voltage excursions.

Fundamental Stability Concepts

- Small/large-signal disturbances
- Linear/nonlinear dynamics

Timescales in Power Systems: Classic

- Classic stability framework - per dominant states:
  - Voltage - Power quality - Automatic voltage regulator (AVR)
  - Angle - Synchronization - Power system stabilizer (PSS)
  - Frequency - Balancing - Inertial response, Primary (droop control, speed governor), secondary (AGC), tertiary.

High-gain AVR can destabilize angle dynamic. To compensate, many generators use power system stabilizer (PSS) to improve damping.

Active power/frequency regulation: If frequency is less than nominal, increase mechanical torque. Vice versa.

AGC adjusts governor setpoints at participating generators: Restores frequency to their scheduled values.

(Higher-level problems: Economic dispatch, Unit commitment)

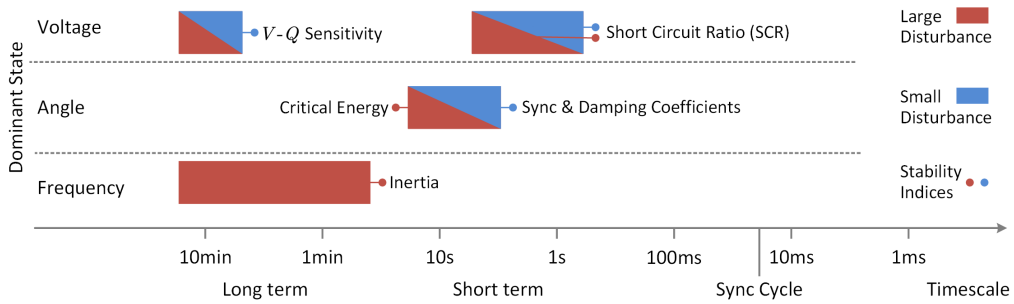

Source: Yunjie Gu, and Timothy C. Green. "Power system stability with a high penetration of inverter-based resources." *Proceedings of the IEEE*, 2022.

IEEE Classification of Power System Stability

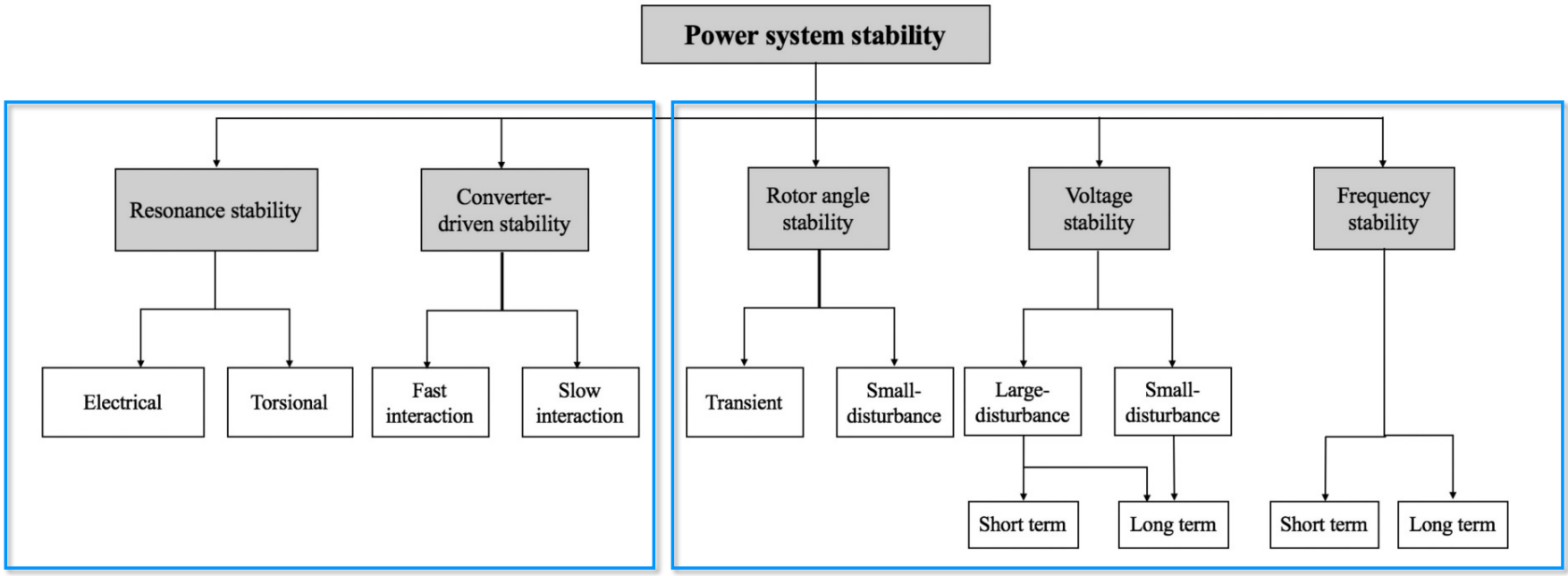

Extension to Future IBR-Dominated Systems

Classic Stability Classification

Source: Stability definitions and characterization of dynamic behavior in systems with high penetration of power electronic interfaced technologies, IEEE Power and Energy Society, Tech. Rep. PES-TR77, May 2020.

Timescales in Power Systems: Future

- New stability framework - Overlaps across time-scale:
  - Electromagnetic dynamics: Instantaneous voltages and currents.
  - Increased speed in frequency dynamics: 1) Reduced inertia of the grid, and 2) Increased response speed of active power from IBRs.
  - Indirect voltage control: Via injecting reactive power to control the terminal voltage amplitude.
  - Inverter inner control loops: Such as PLLs and DC-link voltage control loops.

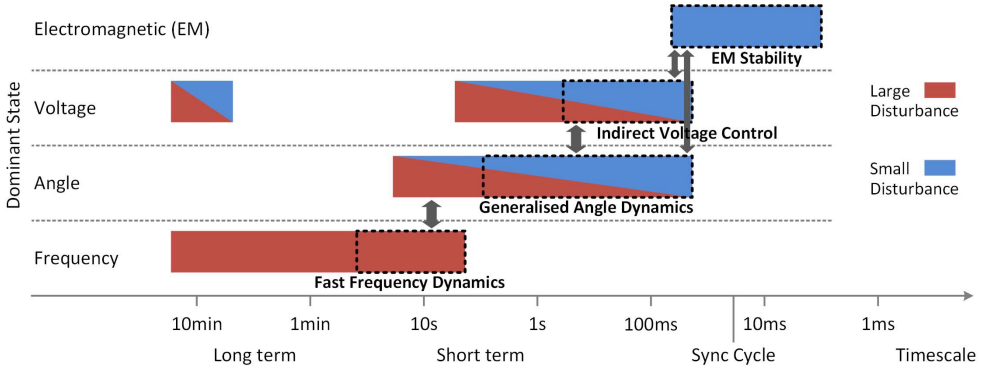

Source: Yunjie Gu, and Timothy C. Green. "Power system stability with a high penetration of inverter-based resources." *Proceedings of the IEEE*, 2022.

Stability Concepts

- Stability is one of the most important property of a dynamical system.
- Fundamental stability concept: Internal (Lyapunov) stability.
- It tells whether the system states can remain close (and converge back) to the equilibrium point (e.p.) after being subjected to a disturbance that perturbs the states away from the e.p.
- Other important stability concepts: BIBO stability, structural stability (bifurcation), solution space boundary.

Why is Power System Stability Difficult?

- Stability is one of the most difficult problem for large-scale complex dynamical systems.
- Linear v.s. nonlinear dynamics (hybrid dynamics)
- Numerical v.s. analytical analysis
  - Challenges in numerical method: Correct model for numerical integration and/or sufficient data; stiff system cause computational burden to assess a large set of interested scenarios; etc.
  - Challenges in analytical method: Inherent difficulty for nonlinear and hybrid systems

Disturbances Across the Temporal Scales

- Stability is inherently associated with disturbances/changes to the system, and the system response.
- Various disturbances: natural environment, equipment failure, operator's actions, system users' actions, malicious actors' actions, system upgrades.

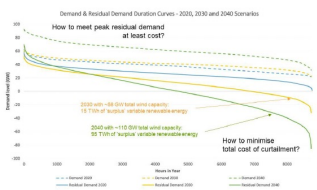

Image: PA
https://inews.co.uk/news/more-than-19000-homes-still-without-power-six-days-after-storm-arwen-1331091

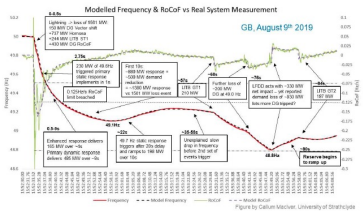

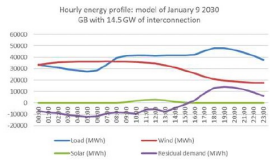

Image: NGESO

Weeks	Days	Minutes	Milliseconds	Microseconds
Energy supply	Network resilience	Ramps of residual demand	Electromechanical stability	Operation of protection System stability with inverters

Source: Keith Bell, "Challenges in setting resilience measures and metrics", CIGRE Group Discussion Meeting, Paris Session, 2022.

Disturbances Across the Physical Scale

- Such disturbance could be "small" or "large" in nature (i.e., how far the disturbance makes the states departure from the equilibrium).
- How small is small and how large is large?
  - For linear systems (i.e., $\dot{x} = f(x)$, f is a linear function of x, denoted by $f = Ax$), the "size" of the disturbance is not important (when it comes to stability). Eigenvalues provide full information about stability. We can talk about a system being stable or unstable, without the need of specifying an e.p.
  - For nonlinear systems (i.e., f is a nonlinear function of x), however, the "size" of the disturbance generally has an influence on whether the states can converge back to the (stable) e.p. or not. And we need to specify which e.p. we are talking about.

"Global Behavior" in Linear Systems

- Qualitative behavior of $x(t)$ for a second order LTI system:

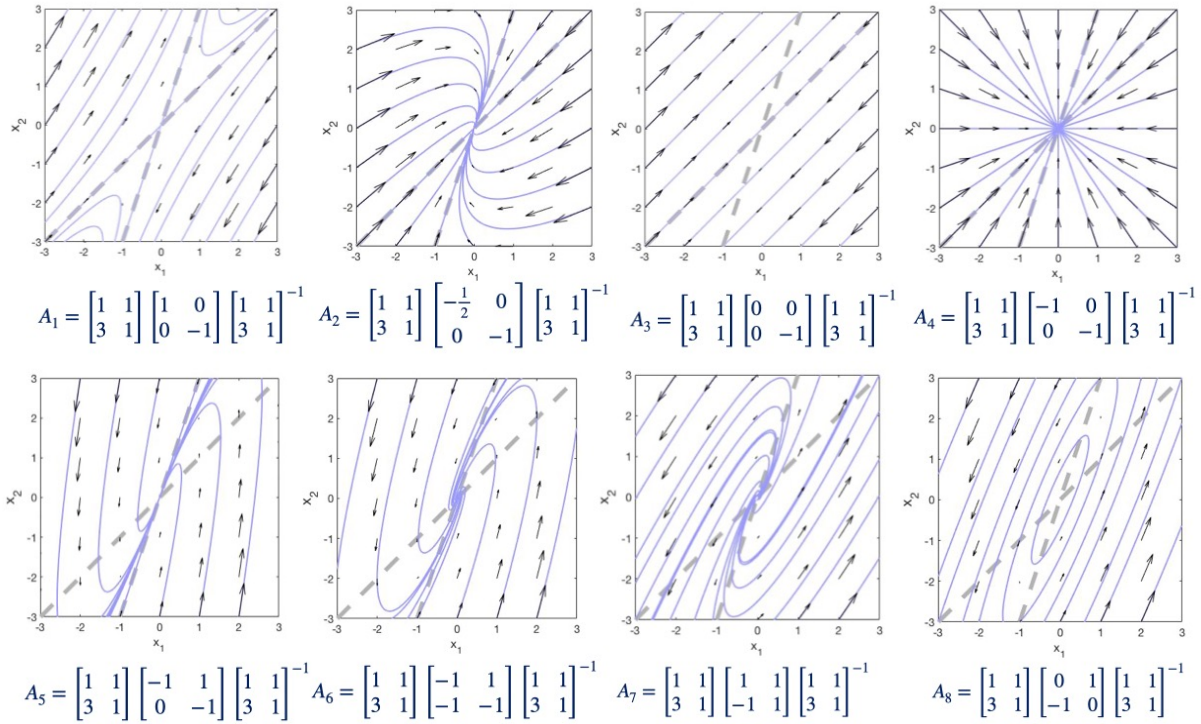

$$A_1 = \begin{bmatrix} 1 & 1 \\ 3 & 1 \end{bmatrix} \begin{bmatrix} 1 & 0 \\ 0 & -1 \end{bmatrix} \begin{bmatrix} 1 & 1 \\ 3 & 1 \end{bmatrix}^{-1} \quad A_2 = \begin{bmatrix} 1 & 1 \\ 3 & 1 \end{bmatrix} \begin{bmatrix} -\frac{1}{2} & 0 \\ 0 & -1 \end{bmatrix} \begin{bmatrix} 1 & 1 \\ 3 & 1 \end{bmatrix}^{-1} \quad A_3 = \begin{bmatrix} 1 & 1 \\ 3 & 1 \end{bmatrix} \begin{bmatrix} 0 & 0 \\ 0 & -1 \end{bmatrix} \begin{bmatrix} 1 & 1 \\ 3 & 1 \end{bmatrix}^{-1} \quad A_4 = \begin{bmatrix} 1 & 1 \\ 3 & 1 \end{bmatrix} \begin{bmatrix} -1 & 0 \\ 0 & -1 \end{bmatrix} \begin{bmatrix} 1 & 1 \\ 3 & 1 \end{bmatrix}^{-1}$$

$$A_5 = \begin{bmatrix} 1 & 1 \\ 3 & 1 \end{bmatrix} \begin{bmatrix} -1 & 1 \\ 0 & -1 \end{bmatrix} \begin{bmatrix} 1 & 1 \\ 3 & 1 \end{bmatrix}^{-1} \quad A_6 = \begin{bmatrix} 1 & 1 \\ 3 & 1 \end{bmatrix} \begin{bmatrix} -1 & 1 \\ -1 & -1 \end{bmatrix} \begin{bmatrix} 1 & 1 \\ 3 & 1 \end{bmatrix}^{-1} \quad A_7 = \begin{bmatrix} 1 & 1 \\ 3 & 1 \end{bmatrix} \begin{bmatrix} 1 & 1 \\ -1 & 1 \end{bmatrix} \begin{bmatrix} 1 & 1 \\ 3 & 1 \end{bmatrix}^{-1} \quad A_8 = \begin{bmatrix} 1 & 1 \\ 3 & 1 \end{bmatrix} \begin{bmatrix} 0 & 1 \\ -1 & 0 \end{bmatrix} \begin{bmatrix} 1 & 1 \\ 3 & 1 \end{bmatrix}^{-1}$$

"Region of Attraction" of Nonlinear Systems

- For nonlinear system, for the post-disturbance states to converge back to an e.p., it requires the following conditions to be met:
  - There exists an e.p.
  - The e.p. must be stable (in the sense of Lyapunov).
  - The post-disturbance point must lie in the stability region (i.e., region of attraction) surrounding that stable e.p. (SEP).

Definition: Stability (of an e.p.) in the sense of Lyapunov:

Consider a system described by $\dot{x} = f(x)$, where f is locally Lipschitz.

- Equilibrium point (e.p.) x^* satisfies $f(x^*) = 0$.
- An e.p. x^* of $\dot{x} = f(x)$ is:
  - Stable, if, for each $\epsilon > 0$ there is a $\delta = \delta(\epsilon) > 0$ such that
    $$\| x(0) \| < \delta \Rightarrow \| x(t) \| < \epsilon, \forall t \geq t_0.$$
  - Unstable if not stable.
  - Asymptotically stable if stable, and δ can be chosen such that $\| x(0) \| < \delta \Rightarrow \lim_{t \to \infty} x(t) = 0$.

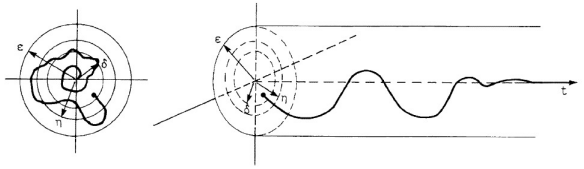

ROA of Classic SMIB Systems

- The swing equation for SMIB system:

$$\dot{\theta} = \omega$$

$$M\frac{d\omega}{dt} + D\omega = P_m - \frac{V_\infty V_t}{X} sin(\theta)$$

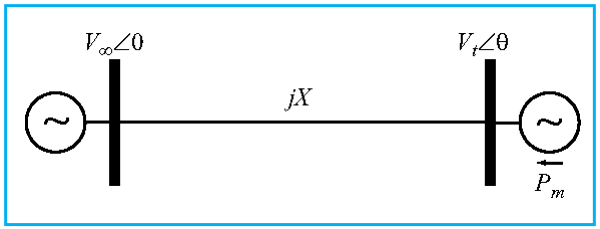

  - Equilibrium conditions: $\omega = 0$ and $P_m = P_{max}sin(\theta)$.
  - Dynamics are similar to a nonlinear pendulum: two e.p., one stable, one unstable.

As P_m increases, ROA shrinks

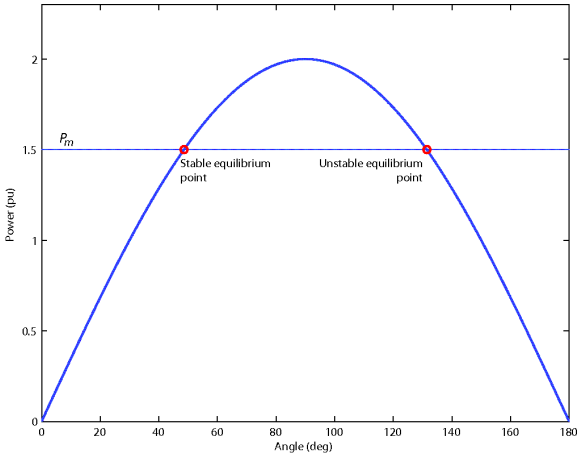

Undamped behavior, $D = 0$

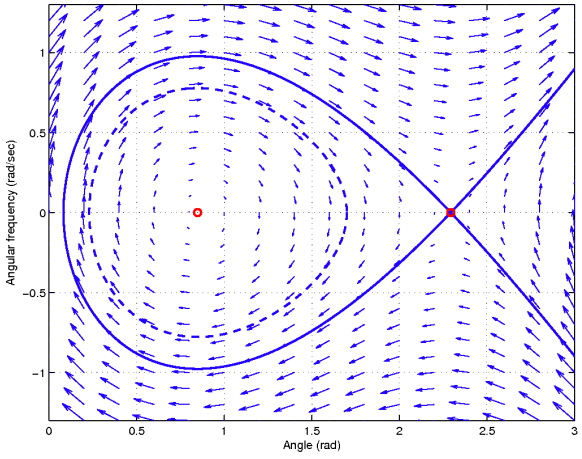

Damped behavior, $D > 0$

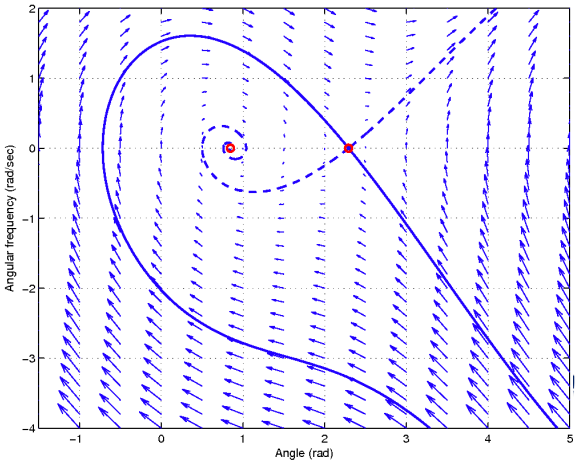

Large Disturbance Behaviors

- A fault/disturbance on the system will force the states away from the stable operating (e.p.) point.
- If the fault is sufficiently large, the disturbance will cause the trajectory to cross the boundary of the region of attraction, and stability will be lost.

ROA of Two-Inverter-Infinite-Bus System

- Models of GFL, GFM and GSP inverters:

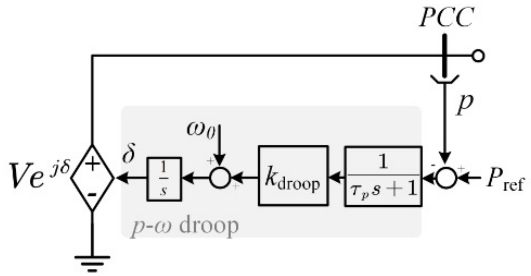

(a) modelling of GFM inverters.

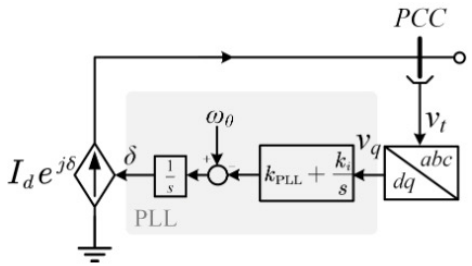

(b) modelling of GFL inverters.

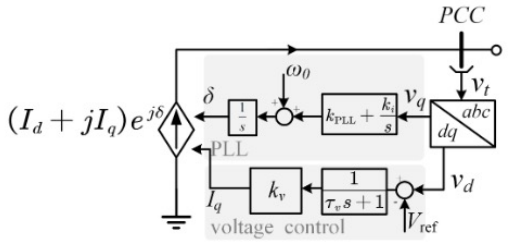

(c) modelling of GSP inverters.

- Two-inverter-infinite-bus system with mixtures of inverter types:

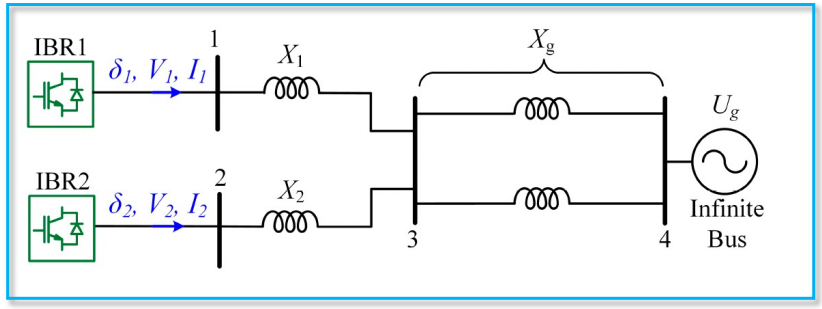

Source: Yifan Zhang, Yaoxin Wang, Yunjie Gu, Sijia Geng, et al. "Large-Signal Stability of Power Systems with Mixtures of GFL, GFM and GSP Inverters.", Preprint.

ROA of Two-Inverter-Infinite-Bus System

- Phase portraits and ROA of two GFL inverters for four test conditions as assessed by a manifold method.

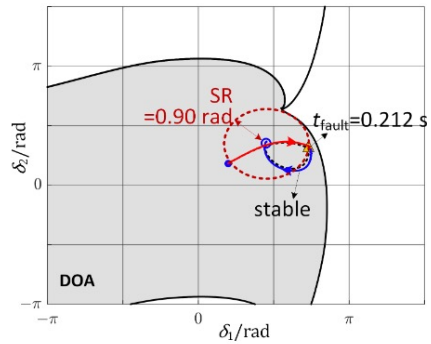

(a) $X_g = 0.35$ p.u., $t_{\text{fault}} = 0.212$ s.

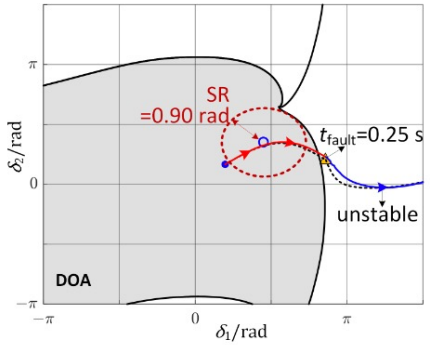

(b) $X_g = 0.35$ p.u., $t_{\text{fault}} = 0.25$ s.

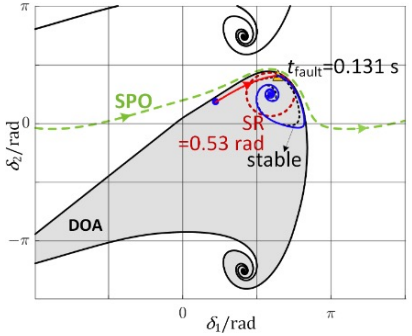

(c) $X_g = 0.4$ p.u., $t_{\text{fault}} = 0.131$ s.

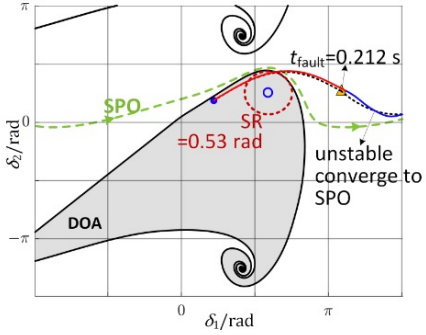

(d) $X_g = 0.4$ p.u., $t_{\text{fault}} = 0.212$ s.

- Solid blue dot: Pre-fault SEP.
- Hollow blue dot: Post-fault SEP
- Yellow triangle: Fault clearance point
- Dashed black line: theoretical (reduced-order model) trajectories. Red lines: EMT simulations during the fault and
- Blue lines: EMT simulations post-fault.
- Green dashed line: Stable periodic orbit.

Source: Yifan Zhang, Yaoxin Wang, Yunjie Gu, Sijia Geng, et al. "Large-Signal Stability of Power Systems with Mixtures of GFL, GFM and GSP Inverters.", Preprint.

Stability Region Estimation Using Energy Function

- Estimate the stability boundary of the system with sub level sets of Lyapunov function.
- This boundary can be used to analyze given faults.
- The stability margin for a given contingency can be estimated.

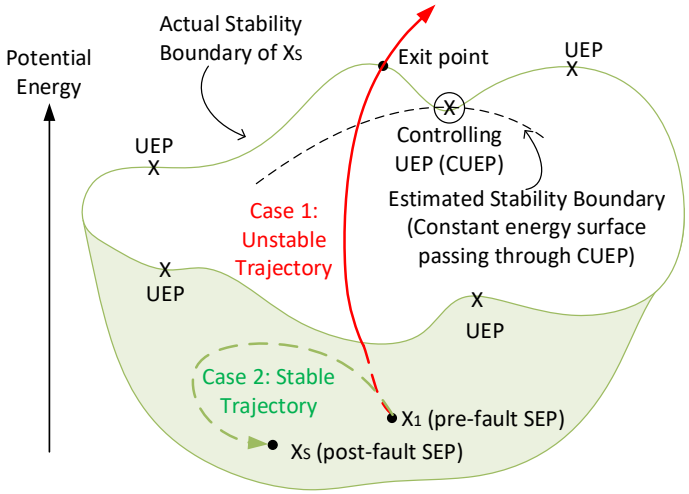

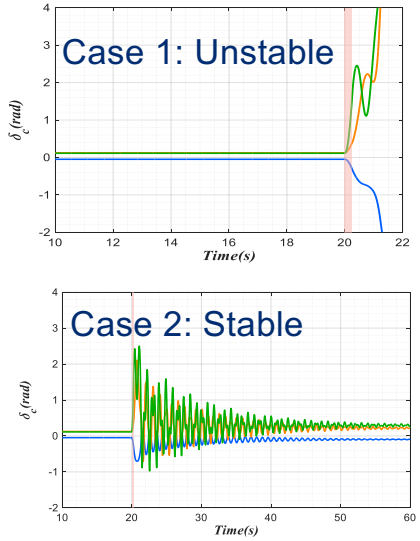

Linearization of Nonlinear Systems

- How can linearization be justified?
- Consider the linear(ized) system $\dot{x} = Ax$ at the equilibrium point x^*, (i.e., $A = \frac{\partial f}{\partial x}|_{x=x^*}$).

Linearization of Nonlinear Systems

- How can linearization be justified?
- Consider the linear(ized) system $\dot{x} = Ax$ at the equilibrium point x^*, (i.e., $A = \frac{\partial f}{\partial x}|_{x=x^*}$).
- Analytical connection between small- and large-disturbance stability:

Theorem: Let $x = 0$ be an e.p. for the nonlinear system $\dot{x} = f(x)$, where f is continuously differentiable near the origin. Let $A = \partial f/\partial x|_{x=0}$. Then:

- The origin is asymptotically stable if all eigenvalues of A have negative real part,
- The origin is unstable if at least one of the eigenvalues of A have positive real part.

Note: We can't determine the stability of the nonlinear system if the linearized system has eigenvalues on the imaginary axis.

Structural Instability and Geometric Interpretation

- **Hopf bifurcation (oscillations)[1,2]**
- **Saddle-node bifurcation (voltage collapse)[3]**

Source:
[1] Sushobhan Chatterjee and Sijia Geng. "Effects of Line Dynamics on the Stability Margin to Hopf Bifurcation in Grid-Forming Inverters." *IREP 2025 and Sustainable Energy, Grids and Networks (SEGAN),* 2025. [2] Sushobhan Chatterjee and Sijia Geng. "Sensitivity to Hopf Bifurcation in Grid-Following Inverters using normal vector methods." *The 60th Annual Allerton Conference on Communication, Control, and Computing,* 2024. **[3]** Sushobhan Chatterjee and Sijia Geng. "Voltage Stability of Inverter-Based Systems: Impact of Parameters and Irrelevance of Line Dynamics." *IEEE PowerTech,* 2025.

Geometric Interpretation of Stability Margin in Parameter Space

- Maintaining stability can be seen as a geometric problem in a multidimensional parameter space to stay away from the stability boundary.
  - $\Sigma \subseteq \mathbb{R}^m$, bifurcation hypersurface, (collects the set of bifurcation points λ_*).
  - Stability margin: $\Delta(\lambda_0) = \|\lambda_* - \lambda_0\|$ (the distance of the nominal parameter to the bifurcation point along direction $k \in \mathbb{R}^m$ in parameter space).
  - Sensitivity: $\Delta_{\lambda_0} = \frac{\partial \Delta(\lambda_0)}{\partial \lambda_0} \in \mathbb{R}^m$ (sensitivity of Δ w.r.t λ_0).
  - Optimal direction: optimal first-order direction of change in λ_0 to increase Δ.

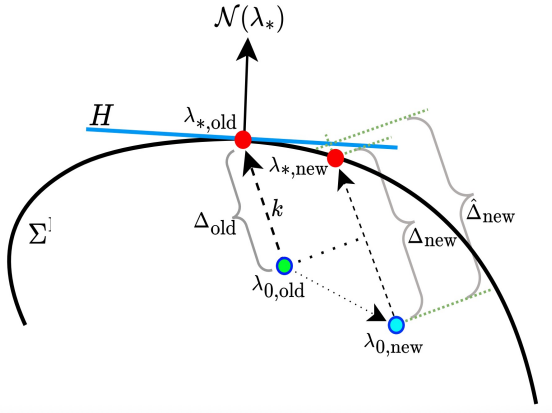

Structural Instability (Bifurcations)

- Bifurcation: Change in the structure of e.p. or periodic orbits, or in their stability properties, as a parameter is varied, i.e., bifurcation parameter.
- Generic local bifurcations: Saddle-Node, Hopf.
  - Saddle-node bifurcation: A real simple eigenvalue crossing over the imaginary axis (Collision of a saddle point and a node). > Voltage collapse
  - Hopf bifurcation: A complex conjugate pair of eigenvalues cross the imaginary axis. > Oscillatory behavior

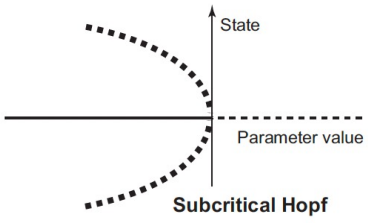

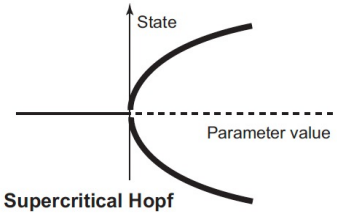

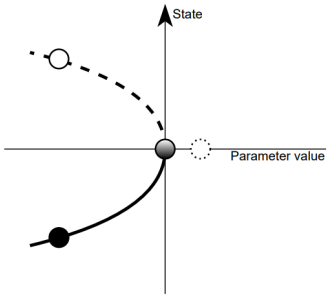

Normal Vectors for Stability Margin Sensitivity

- For Hopf bifurcation, the normal vector is:

$$\mathcal{N}(\lambda_*) = D_\lambda(\Re\{\mu(\lambda)\})|_* = \beta\Re\{w^H(-f_{xx}f_x^{-1}f_\lambda + f_{x\lambda})v\}|_*,$$

where $v_* \in \mathbb{C}^n$ and $w_* \in \mathbb{C}^n$ are the right and left eigenvectors of f_x at $\mu(\lambda_*) = j\omega_*$.

- For saddle-node bifurcation, the normal vector is:

$$\mathcal{N}(\lambda_*) = D_\lambda(\Re\{\mu(\lambda)\})|_* = \alpha w^H f_\lambda|_*; \quad \alpha \neq 0,$$

- Parameter sensitivity: $\Delta_{\lambda_0} = \frac{\partial\Delta(\lambda_0)}{\partial\lambda_0} = -[k^T\mathcal{N}(\lambda_*)]^{-1}\mathcal{N}(\lambda_*)$.

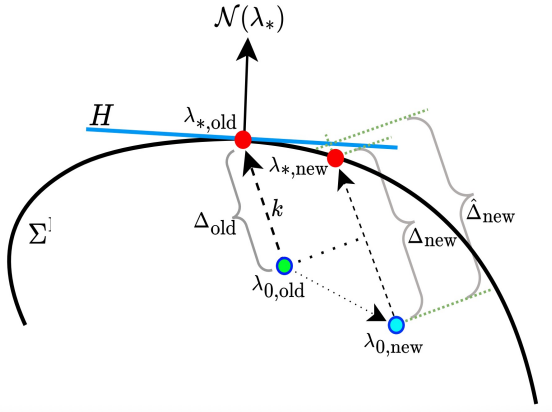

Impacts of Line Dynamics on Stability Margin

Parameter	Nominal value	Margin	
		S-line	D-line
R_f	0.0072 p.u.	3.51733 p.u.	3.49229 p.u.
L_f	0.05 p.u.	3.026723 p.u.	0.1502 p.u.
C_f	0.3 p.u.	✗	✗
ω_{pc}	332.8 rad/s	✗	47.029 rad/s
ω_{qc}	732.8 rad/s	✗	✗
K_P	0.5 %	56.6592 %	0.027295 %
K_Q	0.01 %	✗	0.092975 %
K_{VC}^P	1 p.u.	✗	✗
K_{VC}^I	2.5 p.u.	✗	✗
K_{VC}^F	1 p.u.	1.443487 p.u. p.u.	0.0216725 p.u.
K_{CC}^P	2.5 p.u.	✗	✗
K_{CC}^I	2.5 p.u.	✗	✗
K_{CC}^F	0 p.u.	3.5001035 p.u.	3.4995325 p.u.
ω_0	1 p.u.	✗	✗
V_0	1 p.u.	✗	0.02756 p.u.
p^*	1 p.u.	✗	0.30867 p.u.
q^*	0.5 p.u.	✗	2.756 p.u.
L	0.8 p.u.	✗	0.06132 p.u.
R	0.2 p.u.	✗	0.0182765 p.u.

Hopf stability margin for GFM inverter.

- Important observations:
  - Accounting for line dynamics consistently reduces the Hopf stability margin across parameters for GFM and GFL.
  - It has no impact on S-N stability margin.

Irrelevance of Line Dynamics on S-N Bifurcation

- For a general class of dynamical systems[1], line dynamics are irrelevant for the S-N bifurcation (voltage collapse).
- System setup: IBR connected to an infinite bus via a line.

$$\begin{pmatrix}\dot{x}_1\\ \dot{x}_2\end{pmatrix} = f(x,\lambda) = \begin{pmatrix}h_1(x_1,x_2,\lambda)\\ h_2(x_1,x_2,\lambda)\end{pmatrix}, \qquad x = (x_1, x_2),$$

where $x_1 \in R^{n-q}$ represents the dynamic states of the inverter and $x_2 := (i_{g,D}, i_{g,Q}) \in R^q$ the dynamic states of the line.

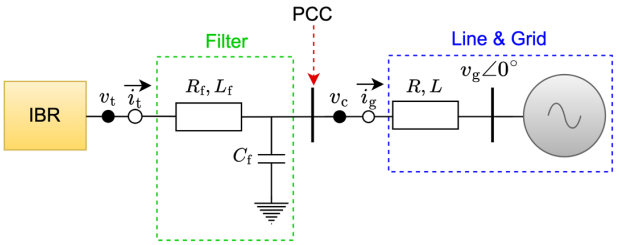

- Jacobian non-singularity:

$$D_{x_2} h_2 = \omega_b \begin{bmatrix} -\frac{R}{L} & \omega_{DQ} \\ -\omega_{DQ} & \frac{R}{L} \end{bmatrix}; \; det \neq 0.$$

Reduced System:

$\dot{x}_1 = \bar{h}(x_1, \lambda) = h_1(x_1, g(x_1, \lambda), \lambda).$

By proposition and IFT, fold bifurcation points remain unchanged under this reduction ⇒ **Line dynamics are irrelevant.**

[1] Dobson et.al. "The irrelevance of electric power system dynamics for the loading margin to voltage collapse and its sensitivities", *Nonlinear Theory and Its Applications,* 2011.

Parameter Sensitivity to Hopf Bifurcations

- The most influential control parameters for GFM to Hopf bifurcation (largest Δ_{λ_0}):

Cause of instability (I)	Static Line		Dynamic Line	
	Control (C)	Sensitivity $\left(\Delta_{\lambda_0}^{C\|I}\right)$	Control (C)	Sensitivity $\left(\Delta_{\lambda_0}^{C\|I}\right)$
$K_P \uparrow$	K_{VC}^F	-144.8507	K_{VC}^F	-1.2503
$K_Q \uparrow$	✗	✗	K_{VC}^F	-4.2547
$\omega_{pc} \uparrow$	✗	✗	K_{VC}^F	-2544
$K_{VC}^F \uparrow$	V_0	3.5683	ω_0	0.8479
$K_{CC}^F \uparrow$	K_{VC}^P	2.5075	K_{VC}^P	2.5084
$R_f \uparrow$	V_0	6.2862	V_0	6.2502
$L_f \uparrow$	K_P	-4.7317	K_{VC}^F	-6.8005
$V_0 \uparrow$	✗	✗	K_{VC}^F	-1.2558
$p^* \downarrow$	✗	✗	K_{VC}^F	22.7076
$q^* \uparrow$	✗	✗	K_Q	-303.9434
$L \downarrow$	✗	✗	K_{VC}^F	2.8449
$R \downarrow$	✗	✗	K_{VC}^F	0.8447

Effective Control Tuning

- Trajectories of active power output ($\tilde{p}$) and voltage (v_c) under various parameter values of K_{VC}^{P} and the bifurcating value of K_{CC}^{F}, for static (upper figures) and dynamic (lower figures) lines.

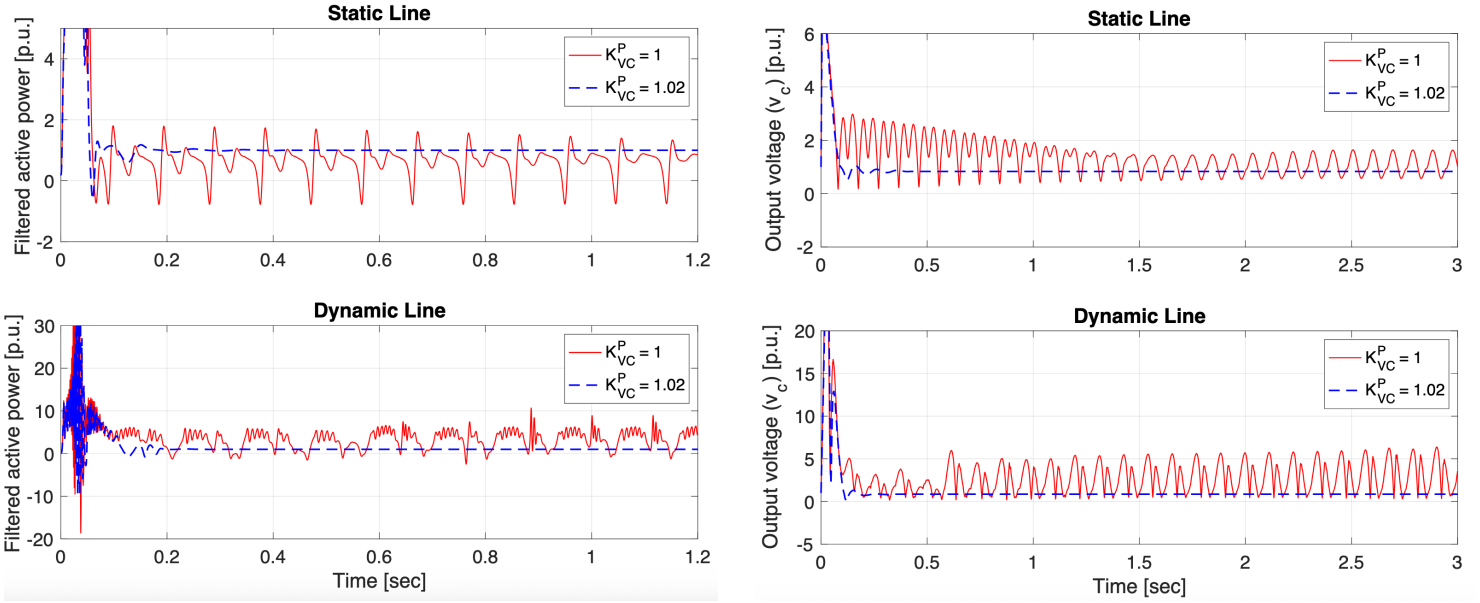

Parameter Sensitivity to S-N Bifurcations

- GFL inverters: Reactive power setpoint q^* is the most effective parameter in countering instabilities due to high active loading, while the feedforward gain of the current controller K_{CC}^F mitigates collapse under high reactive loading. Both findings hold for static and dynamic line models.
- GFM inverters: The feedforward gain of the voltage controller K_{VC}^F is the most influential in stabilizing the system against saddle-node bifurcations from all perturbations. (Interestingly, this is consistent with its efficacy against Hopf bifurcations.)
- Analytical insight: Saddle-node hypersurface remain unchanged when line dynamics are eliminated.

Power System Stability with High Shares of Grid-forming and Grid-following Inverters

II – Advanced Topics

Dr. Sijia Geng, Assistant Professor

Department of Electrical and Computer Engineering

JOHNS HOPKINS UNIVERSITY

DTU PES Summer School
Technical University of Denmark (DTU), Copenhagen, Lyngby, Denmark, May 19, 2026

Outline

Lecture 1 - Fundamentals

- Background of power systems with high shares of inverter-based resources
- Modeling and dynamical responses of GFM and GFL inverters
- Fundamental stability concepts
- (Structural instability)

Lecture 2 – Advanced Topics

- Scale-free decentralized stability and next-generation grid codes
- Safety-critical GFM control with assignable voltage behavior and current limiting
- Singular solution space boundary via differential geometry

Scale-Free Decentralized Stability

- Decentralized stability criteria
- Stability-constrained OPF and economic interpretation of stability service

Centralized Stability Analysis Methods

- Traditional approach for small-signal stability: Eigenvalue computation; Nyquist-based analysis, etc.
- Requires entire system models (state-space or frequency-domain), which are:
  - High-dimensional and nonlinear, especially in multi-converter systems.
  - Dependent on operating points and network topology.
- Increasing shares of heterogeneous power electronics-based devices make global analysis challenging.

Why Centralized Analysis Fails to Scale?

- Significant fluctuations in operating conditions:
  - Robust to operating point variation.
- Increased system complexity and nonlinearity:
  - Scalable to detailed modeling of numerous IBRs.
- Adding and removing devices to the grid:
  - Adaptive to plug-and-play.
- Lack of transparency in control implementations:
  - Decentralized approach that only needs local information, to be checked by individual devices, yet ensure system-level stability.

Decentralized Stability Criteria

- **Interconnection:**

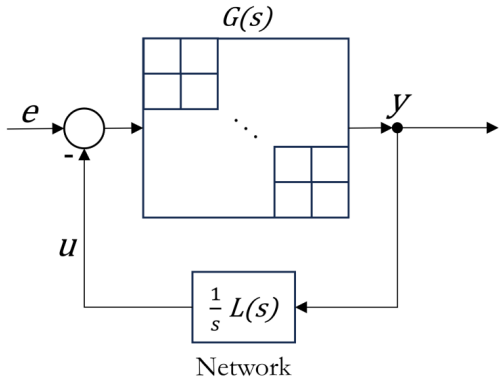

- **System equations:**

$$y_i(s) = g_i(s)(e_i(s) - u_i(s))$$
$$u(s) = \frac{1}{s} L y(s).$$

- **Standard approach: passivity**

Assume: $g_i(s)$ is strictly passive
Test: The interconnection is stable if network model L satisfies $L \in \mathcal{L} = \{L : L = L^T, 0 \preceq L \preceq I\}$.

- **Exploit limited network info, extend passivity condition:**

Assume: $g_i(s)$ is stable
Define: *h*(*s*) ∈ *Positive Real*
Test: If $\forall i, \exists 0 \leq \gamma \leq 1$, such that, $h(s)(1 + \gamma g_i(s)/s) \in ESPR$, then the system is stable for network $L \in \mathcal{L} = \{L : L = L^T, 0 \preceq L \preceq I\}$.

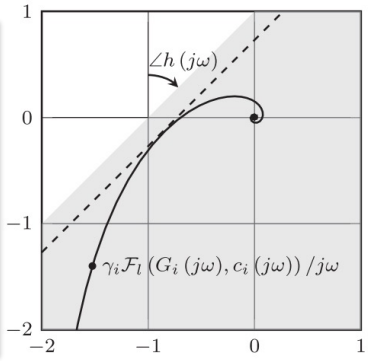

Source: Richard Pates and Enrique Mallada, "Robust scale-free synthesis for frequency control in power systems," IEEE Transactions on Control of Network Systems, (2019).

Power System Model as Feedback Interconnection

- **Network model: Linearized fast-decoupled power flow.**

$$\mathrm{vec}\left(\left\{\begin{bmatrix}\Delta P_i\\ \Delta Q_i\end{bmatrix}\right\}_{i\in\mathcal{V}}\right) = \frac{1}{s} L_B \,\mathrm{vec}\left(\left\{\begin{bmatrix}\Delta\dot{\theta}_i\\ \Delta\dot{v}_i\end{bmatrix}\right\}_{i\in\mathcal{V}}\right)$$

- Transmission lines are lossless.
- At equilibrium, the angle difference across each transmission line is small.
- Transient voltage magnitudes lie in $[V_{min}, V_{max}]$.

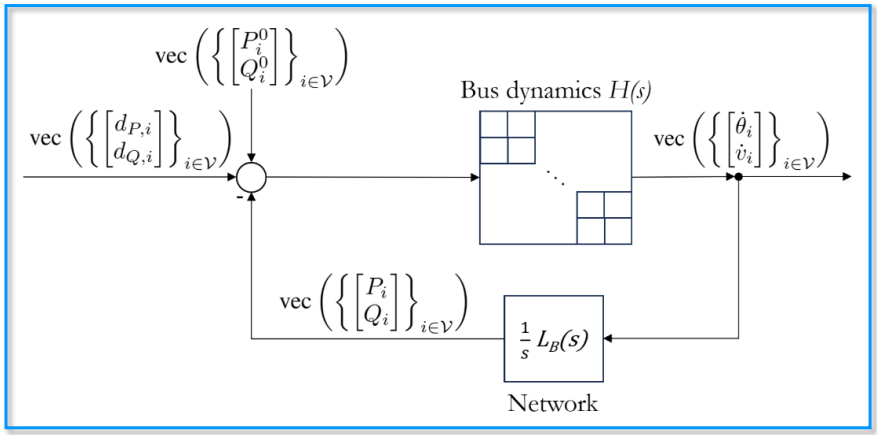

where "Decoupled linearized power flow"

$$L_B = \begin{bmatrix} \tilde{P}_{\theta,11} & 0 & \dots & \tilde{P}_{\theta,1N} & 0 \\ 0 & \tilde{Q}_{v,11} & \dots & 0 & \tilde{Q}_{v,1N} \\ \vdots & \vdots & \ddots & \vdots & \vdots \\ \tilde{P}_{\theta,N1} & 0 & \dots & \tilde{P}_{\theta,NN} & 0 \\ 0 & \tilde{Q}_{v,N1} & \dots & 0 & \tilde{Q}_{v,NN} \end{bmatrix}$$

and

$$\tilde{P}_{\theta,ij} = \frac{\partial}{\partial\theta_j} \sum_{l\in\mathcal{N}_i} -v_i v_l b_{il} \sin(\theta_i - \theta_l)\Big|_{\theta=\theta_0, v=V_0}$$

$$= \begin{cases} -\sum_{l\in\mathcal{N}_i} V_{0i} V_{0l} b_{il} \cos(\theta_{0i} - \theta_{0l}), & i = j, \\ V_{0i} V_{0j} b_{ij} \cos(\theta_{0i} - \theta_{0j}), & i \neq j, \end{cases}$$

$$\tilde{Q}_{v,ij} = \frac{\partial}{\partial v_j} \left(v_i^2 b_{ii} + \sum_{l\in\mathcal{N}_i} v_i v_l b_{il} \cos(\theta_i - \theta_l) \right)\Big|_{\theta=\theta_0, v=V_0}$$

$$= \begin{cases} 2V_{0i} b_{ii} + \sum_{l\in\mathcal{N}_i} V_{0l} b_{il} \cos(\theta_{0i} - \theta_{0l}), & i = j, \\ V_{0i} b_{ij} \cos(\theta_{0i} - \theta_{0j}), & i \neq j. \end{cases}$$

Source: Zudika Siahaan, Enrique Mallada, and Sijia Geng. "Decentralized stability criteria for grid-forming control in inverter-based power systems." The Proceedings of 2024 IEEE PES General Meeting.

Decentralized Stability Criteria: Grid-Code

- Power system model:

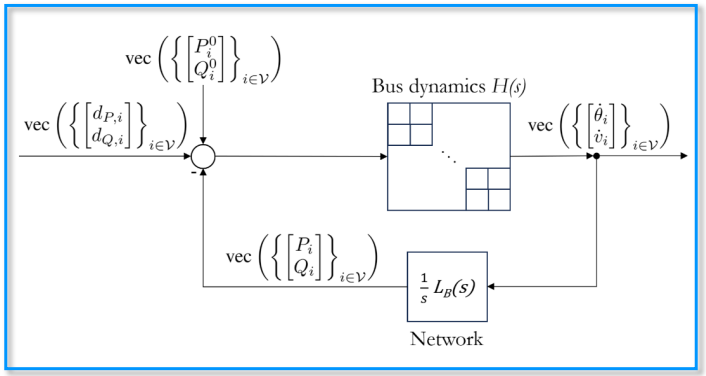

Bus dynamics: Droop-based GFM IBR

$$\begin{cases} \dot{\theta}_i &= \omega_i \\ \omega_i &= \omega_i^0 + m_i^p f_i^p(s)(P_i^0 - P_i), \\ v_i &= V_i^0 + m_i^q f_i^q(s)(Q_i^0 - Q_i). \end{cases}$$

$$h_i^\theta = \frac{m_i^p \beta_i^p / \tau_i^p}{s + 1/\tau_i^p} \qquad h_i^v = \frac{s m_i^q \beta_i^q / \tau_i^q}{s + 1/\tau_i^q}$$

Theorem

Given the feedback interconnection on the left consisting of synchronous machines and droop-controlled GFM IBRs, with the droop constants $m_i^p, m_i^q \in \mathbb{R}_{\geq 0}$ and the filter's time constants $\tau_i^p, \tau_i^q \in \mathbb{R}_{>0}$. Then the system is stable whenever each controller gain satisfies,

$$\left(\max_{j \in \mathcal{N}_i}\{V_{0j}\} - V_{0i}\right) \beta_i^q m_i^q \leq \frac{1}{2|b_{ii}|}, \quad \forall i \in \mathcal{V}.$$

(+) Condition relies solely on local information
(+) Employ the least conservative decentralized framework
(+) Apply MIMO transfer functions
(-) Implement homogeneous model of GFM control
(-) Based on static lossless decoupled network model

GFM inverter is vulnerable to strong grids. (high $|b_{ii}|$)

Source: Zudika Siahaan, Enrique Mallada, and Sijia Geng. "Decentralized stability criteria for grid-forming control in inverter-based power systems." The Proceedings of 2024 IEEE PES General Meeting.

Conservativeness of the Decentralized Criteria

- Gap of the decentralized criteria versus eigenvalue-based criteria.

$$\left(\max_{j\in\mathcal{N}_i}\{V_{0j}\}-V_{0i}\right)\beta_i^q m_i^q \le \frac{1}{2|b_{ii}|}, \quad \forall i\in\mathcal{V}.$$

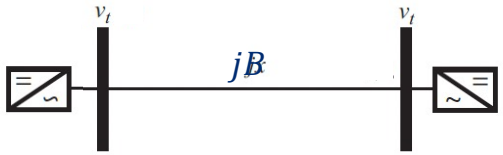

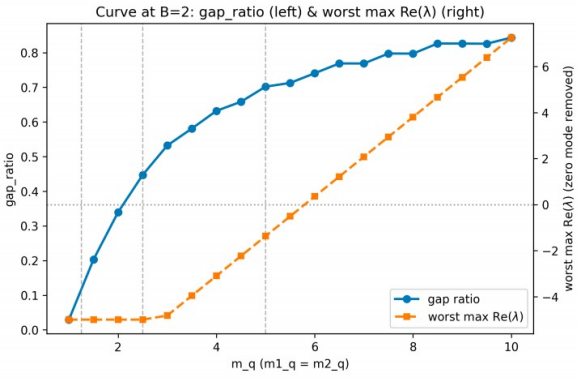

(a) $B = 2$

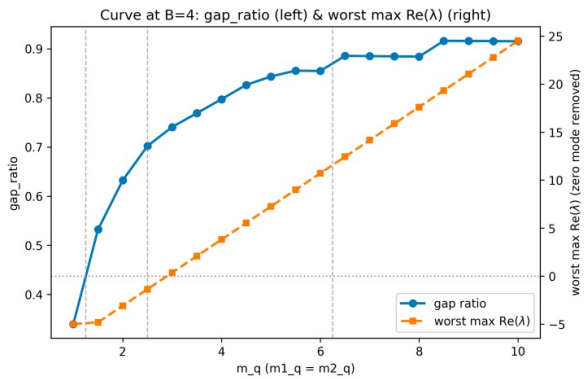

(c) $B = 4$

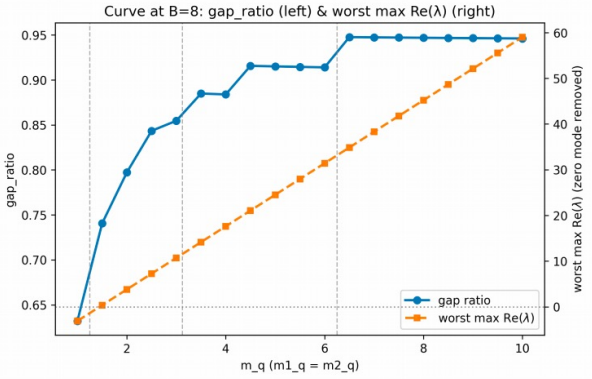

(e) $B = 8$

Conservative (sufficient condition) but meaningful (i.e., robustness)

Operation Model v.s. Dynamical Model

- Operation model: Feasibility and optimality.

$$\begin{aligned} &min\, J(y) \\ &s.t.\ 0 = g(y), \\ &\quad 0 > h(y). \end{aligned}$$

Power flow equations

Constraints on voltage, power, and thermal

- Dynamical model: Stability and control.

$$\begin{aligned} &\dot{x} = f(x, y), \\ &0 = g(x, y). \end{aligned}$$

Dynamical equations

Static equations

- Why stability should be considered at the operational level
  - More stressed condition; closer to stability boundary.
  - Higher variability of operating points.

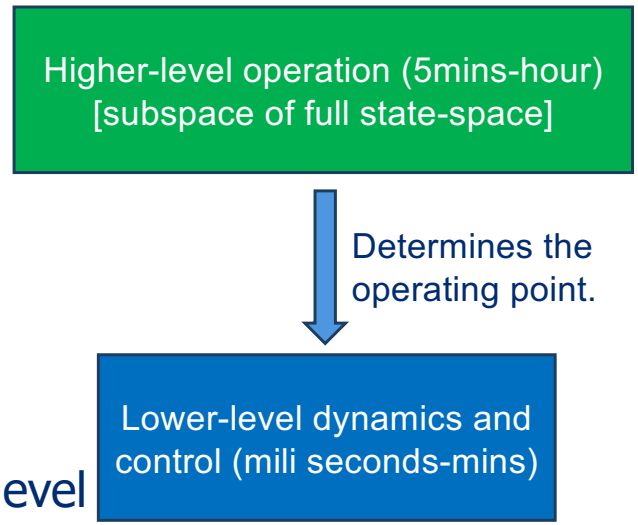

Stability-Constrained OPF

- Existing approaches:
  - Aggregated performance metrics: such as ROCOF, Nadir, etc.
  - Abstracted metrics: SCR, etc.
  - Eigenvalue-based stability: global model, no analytical expression.
  - Hierarchical numerical evaluations: time-consuming.

- Challenges:
  - Approximated stability characterization.
  - Numerical complexity.
  - Lack of interpretation of the economic value of stability service for individual devices.

Decentralized Stability-Constrained OPF

- Key formulation: Individual stability constraint for each IBRs to ensure system-level (small-signal) stability.
- Advantages:
  - Sufficient condition.
  - Analytical form and easy to interpret the value of stability provision from individual devices: Nodal Stability Shadow Prices (NSSP):

$$\lambda_i^{\text{stab}} := \sum_{j \in \mathcal{N}_i^{\text{red}}} \lambda_{ij}^{\text{stab}}$$

$$\begin{aligned}
(\mathcal{P}_1) \quad & \min_{\{P_{Gi}, Q_{Gi}, \theta_i, V_i\}} \; J_{\text{obj}} = \sum_{i=1}^{2} \left(c_i P_{Gi}^2 + b_i P_{Gi} + a_i\right) \\
\text{s.t.} \quad & \theta_1 = 0, \\
& P_{G1} - P_{D1} = -V_1 V_2 B \sin\theta_2, \\
& P_{G2} - P_{D2} = V_2 V_1 B \sin\theta_2, \\
& Q_{G1} - Q_{D1} = V_1^2 B - V_1 V_2 B \cos\theta_2, \\
& Q_{G2} - Q_{D2} = V_2^2 B - V_1 V_2 B \cos\theta_2, \\
& (line - flow \; and \; box \; constraints \; on \; P_{Gi}, Q_{Gi}, V_i), \\
& V_2 - V_1 \le \Gamma_1, \\
& V_1 - V_2 \le \Gamma_2.
\end{aligned}$$

Source: Shigeng Wang and Sijia Geng. "Decentralized Stability-Constrained Optimal Power Flow for Inverter-Based Power Systems." arXiv preprint: https://doi.org/10.48550/arXiv.2604.17603.

Key Theoretical Questions

- *Does (decentralized) stability constraints affect OPF decisions?*
- *When does it induce trade-offs?*
- *What is the economic value of stability service? Is stability provision costly?*

Result 1: Stability Can be "Free"

Conditions:

- Lossless network $P_i^{\text{net}} = \sum_j V_i V_j B_{ij} \sin(\theta_i - \theta_j), \qquad Q_i^{\text{net}} = -V_i^2 B_{ii} - \sum_{j \neq i} V_i V_j B_{ij} \cos(\theta_i - \theta_j)$
- P-only objective $x := (P_G, Q_G, V, \theta), \qquad \theta_1 = 0, \qquad J(P_G) = \sum_{i=1}^{n} (c_i P_{Gi}^2 + b_i P_{Gi} + a_i)$
- Voltage-difference stability criteria $h_\ell(V) := \alpha_\ell^\top V \leq \Gamma_\ell, \qquad \ell = 1, \ldots, L, \qquad \text{with } \alpha_\ell^\top \mathbf{1} = 0$

Theorem 1. (Voltage-difference stability constraints binding with zero shadow prices with P-only objective)

Let $x^\star$ be a KKT point of the OPF problem where only the voltage-difference stability constraints are binding. Let

$$\mathcal{A} := \{\ell : h_\ell(V^\star) = \Gamma_\ell\}$$

denote the active set. Assume that the active constraint vectors $\{\alpha_\ell\}_{\ell \in \mathcal{A}}$ are positively linearly independent, i.e., they admit no nontrivial nonnegative linear combination equal to zero. Then the associated multipliers satisfy

$$\rho_\ell^\star = 0, \qquad \forall \ell \in \mathcal{A}.$$

Stability constraint may be active but has zero shadow price.

Result 1: Stability Can be "Free"

Proof:

Lagrangian: $\mathcal{L} = J(P_G) + \lambda_P^\top (P_G - P_D - P^{\text{net}}) + \lambda_Q^\top (Q_G - Q_D - Q^{\text{net}}) + \sum_{\ell=1}^{L} \rho_\ell (\alpha_\ell^\top V - \Gamma_\ell).$

Step 1. $\dfrac{\partial \mathcal{L}}{\partial Q_G} = \dfrac{\partial J}{\partial Q_G} + \lambda_Q = 0 \quad \Rightarrow \quad \lambda_Q = 0$ **(objective has no Q)**

Step 2. $\dfrac{\partial \mathcal{L}}{\partial \theta_i} = -\sum_j (\lambda_{Pi} - \lambda_{Pj}) V_i V_j B_{ij} \cos(\theta_i - \theta_j) = 0 \quad \forall i \quad \Rightarrow \quad \lambda_{Pi} = \lambda_{Pj}, \quad \forall i, j,$ **(λ_P is uniform)**

Step 3. $\dfrac{\partial \mathcal{L}}{\partial V} = \underbrace{-\nabla_V (\lambda_P^\top P^{\text{net}})}_{\in \text{span}\{\mathbf{1}\}} \underbrace{- \nabla_V (\lambda_Q^\top Q^{\text{net}})}_{0} + \sum_{\ell=1}^{L} \rho_\ell \alpha_\ell = 0$

$\Rightarrow \quad -\nabla_V (\lambda_P^\top P^{\text{net}}) = 0, \qquad \sum_{\ell=1}^{L} \rho_\ell \alpha_\ell = 0.$

$\sum_{\ell=1}^{L} \rho_\ell \alpha_\ell \in \mathcal{D} := \{v \in \mathbb{R}^n : \mathbf{1}^\top v = 0\} \perp \text{span}\{\mathbf{1}\}$

Step 4. $\sum_{\ell \in \mathcal{A}} \rho_\ell \alpha_\ell = 0, \qquad \rho_\ell \geq 0 \quad \Rightarrow \quad \rho_\ell = 0, \qquad \forall \ell \in \mathcal{A}$

Positive linear independence

Result 2: When Stability Matters – Opportunity Cost of Q

- Independent binding with positive shadow price requires structural conditions

$$f(P,Q;\alpha) = \sum_{i=1}^{n}(c_i P_{Gi}^2 + b_i P_{Gi}) + \sum_{i=1}^{n} d_i Q_{Gi}^2, \quad \textit{parameterized by } \alpha \in \mathbb{R}^{3n}.$$

Theorem 2. (Necessary condition for independent binding with positive shadow price)

Consider an AC OPF problem with equality constraints $g(x) = 0$ and inequalities $h_i(x) \geq 0$, including a stability constraint h_s. Let x^* be a local optimum where h_s is the only active inequality. Assume the Linear Independence Constraint Qualification (LICQ) holds at x^*, i.e., the active constraint gradients are linearly independent. Then a necessary condition for h_s to be independently binding with positive shadow price is that there exist α and $\mu_s > 0$ such that

$$A(x^*)\alpha + \mu_s \nabla_z h_s(z^*) = 0.$$

Stability becomes economically relevant
when it conflicts with optimal dispatch.

Result 3: Sufficient Condition for When Stability Matters

- Necessary + Second order sufficient condition (SOSC) → sufficient
- Nonzero shadow price guaranteed

Theorem 3. (Sufficient condition for independent binding with positive shadow price)

Under the same setting as Theorem 2, suppose there exist α *and* $\mu_s > 0$ *such that* $A(x^*)\alpha + \mu_s \nabla_z h_s(z^*) = 0$. *Furthermore, suppose that the second-order sufficient condition (SOSC) holds at* x^*, *i.e., the Lagrangian Hessian is positive definite on the critical cone of* $\{g, h_s\}$. *Then* x^* *is a strict local minimizer, and the stability constraint* h_s *is independently binding with positive shadow price at* x^*.

A complete characterization of when stability induces trade-offs.

Case: Stability–Optimality Trade-Off

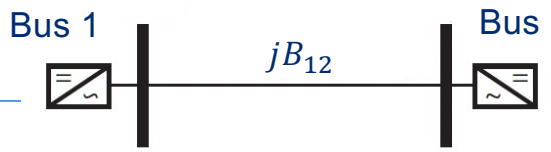

Variables: P_{G1}, Q_{G1} $P_{G2}, Q_{G2}, V_2, \theta_2$

Known: $P_{D1}, Q_{D1}, \theta_1, V_1$ P_{D2}, Q_{D2}

Setup:

- 2-bus lossless AC OPF
- Objective includes P and Q cost terms
- Voltage-difference stability criteria $|V_1 - V_2| \le \Gamma, \quad \Gamma = \dfrac{1}{2m_i^q \beta_i^q |B_{ii}|} > 0$

Case	Γ	$\lvert V_1 - V_2 \rvert$	Obj. J	ΔJ (vs Base)	ρ_s	Independent Binding?
Base	0.040000	0.040000	1.400923	0.000000	8.0483	Yes
Relax	0.042000	0.042000	1.387804	-0.013120	5.0701	Yes
Remove	–	0.045391	1.379200	-0.021724	–	No

Independently binding stability constraint for individual IBR is priced.

Takeaways

- Decentralized small-signal stability criteria
- Decentralized stability-constrained OPF
- Stability is not always costly (reflects formulation limitation)
- When it is, we can quantify it
- Opportunity cost of reactive power from IBRs

Safety-Critical Grid-Forming Control

Assignable voltage regulation guarantees and safety-critical current limiting

Source: Bhathiya Rathnayake and Sijia Geng, "Grid-Forming Control with Assignable Voltage Regulation Guarantees and Safety-Critical Current Limiting," arXiv preprint arXiv:2603.02975, 2026

The Grid is Being Rebuilt — Controllers are Centric Now

- The important control problems

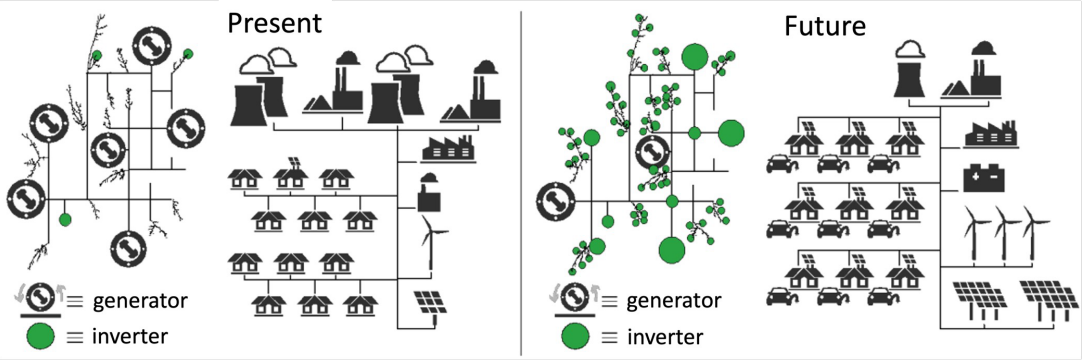

What's changing

Synchronous generators (rotating, slow) → power electronics (fast, software-controlled).

What this costs us

Inertia, fault current, and the natural voltage source behavior of physical machines — all gone unless we put them back via control.

Source: Y. Lin et al., "Research roadmap on grid-forming inverters," Nat. Renew. Energy Lab., Golden, CO, USA, Tech. Rep. NREL/TP-5D00-73476, Nov. 2020.

Safety-critical grid-forming control:

Voltage source behavior – Grid-Forming

Make the inverter act like a voltage source —**form the voltage waveform**— under *unknown grid conditions* and *unknown line impedance*.

Current Limits – Strict Safety Constraints

Inverter terminal current must **NEVER** exceed ~1.2 p.u. — *semiconductors burn out*. Synchronous generators tolerate 5–7 p.u.; we don't have that margin.

IBR Connected to the Grid

- VSC + LCL filter + (unknown) transmission line + unknown grid voltage

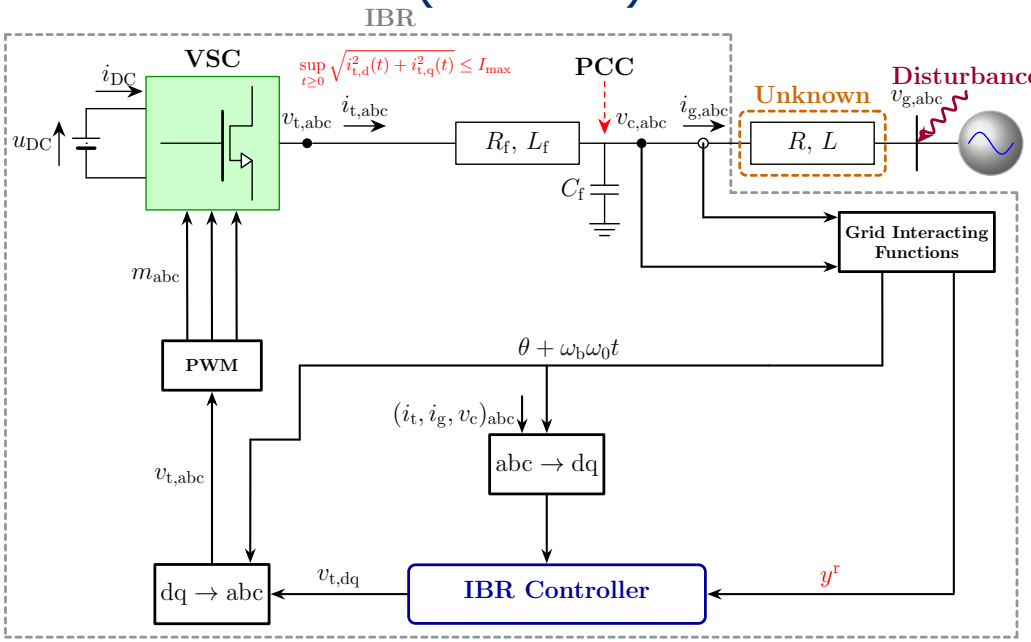

System schematic

State (electrical)

$\boldsymbol{x}_{inv} = \left[i_{t,d}, i_{t,q}, v_{c,d}, v_{c,q}, i_{g,d}, i_{g,q}\right]^T \in \mathbb{R}^6$

Control input

$\boldsymbol{v}_t = \left[v_{t,d}, v_{t,q}\right]^T$

Outputs to regulate

PCC voltage $(v_{c,d}, v_{c,q}) \rightarrow$ droop-generated reference $(v_{c,d}^r, 0)$

Disturbance / uncertainty

Grid voltage $v_{g,d}, v_{g,q} \in L^\infty$ (*bound unknown*).
Line $R, L > 0$ *unknown constants*.

Safety constraint (hard)

$\|\boldsymbol{i}_t(t)\| \leq I_{max}$ for all $t \geq 0$

Here

$\boldsymbol{i}_t = \left[i_{t,d}, i_{t,q}\right]^T$

Architecture: Droop + Backstepping (BS) Nominal Control

- Standard inner/outer loop architecture; nonlinear robustness inside

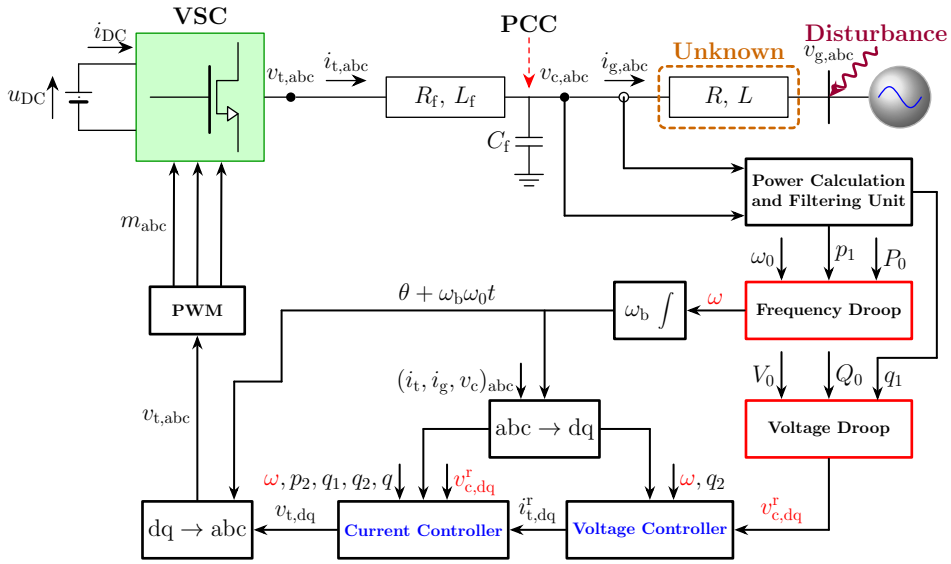

Droop & control loops

1 Droop Laws

Freq. Droop: Active power → frequency,

$$\omega = \omega_0 + K_P(P_0 - p_1)$$

Volt. Droop: Reactive power → voltage reference.

$$v^r_{c,d} = V_0 + K_Q(Q_0 - q_1) \qquad v^r_{c,q} = 0$$

2 Voltage controller (BS virtual control)

Pick reference current $i^r_{t,dq}$ to drive $v_{c,dq} \to v^r_{c,dq}$.

d-axis

$$i^r_{t,d} = i_{g,d} - C_f\omega v_{c,q} - \left(\frac{C_f K_Q}{\omega_b}\right) q_2 - \left(\frac{C_f K_{VC}}{\omega_b}\right)(v_{c,d} - v^r_{c,d})$$

3 Current controller (BS + DADS)

Synthesize $v_{t,dq}$ to drive $i_{t,dq} \to i^r_{t,dq}$.

d-axis

$$v_{t,d} = \left(\frac{L_f}{\omega_b}\right)\left(\begin{array}{c}\text{nonlin. cancel.} + \text{error\_term1}(i_{t,d} - i^r_{t,d}) \\ + \text{error\_term2}(v_{c,d} - v^r_{c,d}) + u_d\end{array}\right)$$

Nonlinear damping with adaptive gain handles unknown $v_{g,dq}$ and unknown R, L.

Deadzone-Adapted Disturbance Suppression (DADS)

- See more at Robust Adaptive Control, Karafyllis & Krstic, 2025

1 **Nonlinear damping with adaptive gain (d-axis)**

$$u_{\mathrm{d}} = -\left(\frac{(1 + \mathrm{e}^{z_{\mathrm{d}}})\omega_{\mathrm{b}}^2}{4}\left(1 + i_{\mathrm{g,d}}^2 + v_{\mathrm{c,d}}^2\right)\right)\left(i_{\mathrm{t,d}} - i_{\mathrm{t,d}}^{\mathrm{r}}\right)$$

Bigger error signals → more damping injected.

2 **Deadzone on the adaptation law (d-axis)**

$$\dot{z}_{\mathrm{d}} = \Gamma_{\mathrm{d}} e^{-z_{\mathrm{d}}} \max\{W_{\mathrm{d}} - \varepsilon, 0\}, \qquad W_{\mathrm{d}} = \frac{1}{2}\left(v_{\mathrm{c,d}} - v_{\mathrm{c,d}}^{\mathrm{r}}\right)^2 + \frac{1}{2}\left(i_{\mathrm{t,d}} - i_{\mathrm{t,d}}^{\mathrm{r}}\right)^2$$

Adaptive gain z_{d} only grows when error energy W_{d} exceeds threshold ε. This is the key to preventing gain drift — a classical pathology of adaptive control.

3 **What you get**

Tunable residual: $\limsup_{t\to\infty}\left|v_{\mathrm{c,dq}}(t) - v_{\mathrm{c,dq}}^{\mathrm{r}}(t)\right| \le \sqrt{2\varepsilon}$ — independent of $\|v_{\mathrm{g,dq}}\|_\infty$ and of R, L. Boundedness of all states including $z_{\mathrm{d,q}}$.

Pick ε small → arbitrarily small ultimate error. Pay for it in control effort. No bound on $v_{\mathrm{g,dq}}$ needed in design.

Safety: Hard Current Limit via Control Barrier Function

- Forward-invariance of $\|\boldsymbol{i}_t\| \leq I_{max}$

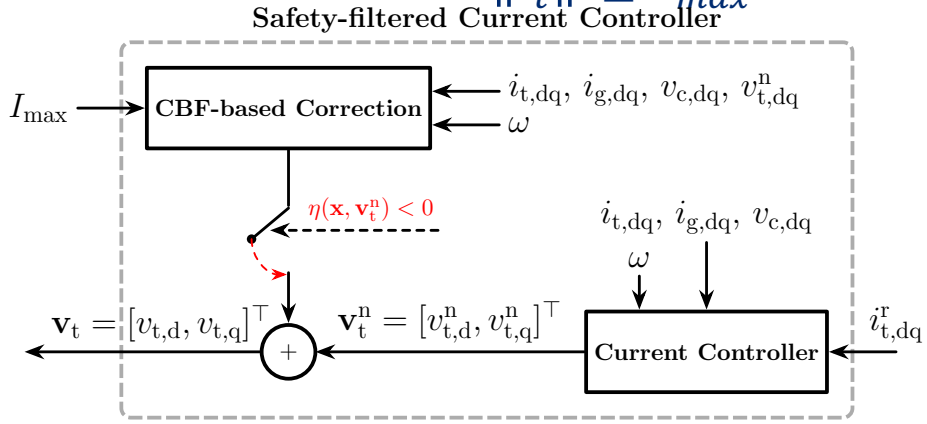

Safety filter wraps the nominal control

What we get

For ***any*** locally Lipschitz nominal $\boldsymbol{v}^{\mathrm{n}}_{\mathrm{t}}$,

$$\|\boldsymbol{i}_{\mathrm{t}}(t)\| \leq I_{max}, \qquad \forall\, t$$

All remaining states $v_{\mathrm{c,dq}}, i_{\mathrm{g,dq}}, z_{\mathrm{dq}}$, and power filter states are bounded.

Barrier function

$h(\boldsymbol{x}) = I_{\max} - \|\boldsymbol{i}_{\mathrm{t}}\|^2$; $\quad \boldsymbol{i}_{\mathrm{t}} = [i_{\mathrm{t,d}}, i_{\mathrm{t,q}}]^{\mathrm{T}}$

Safe set: $\mathcal{C} = \{\boldsymbol{x} \in \mathbb{R}^{10} : h(\boldsymbol{x}) \geq 0\}$

CBF condition

$\dot{h}(\boldsymbol{x}, \boldsymbol{v}_{\mathrm{t}}) \geq -c\, h(\boldsymbol{x})$; $\quad \boldsymbol{v}_{\mathrm{t}} = [v_{\mathrm{t,d}}, v_{\mathrm{t,q}}]^{\mathrm{T}}$

$\Rightarrow\ h(t) \geq e^{-ct}\, h(0) \geq 0$

Affine in $\boldsymbol{v}_{\mathrm{t}}$

$$\min_{\boldsymbol{v}_{\mathrm{t}}} \|\boldsymbol{v}_{\mathrm{t}} - \boldsymbol{v}^{\mathrm{n}}_{\mathrm{t}}\| \ s.t.\ \ \dot{h}\,(\boldsymbol{x}, \boldsymbol{v}_{\mathrm{t}}) \geq -c\, h(\boldsymbol{x})$$

Closed-form solution

$$\boldsymbol{v}_{\mathrm{t}} = \begin{cases} \boldsymbol{v}^{\mathrm{n}}_{\mathrm{t}}, & \eta(\boldsymbol{x}, \boldsymbol{v}^{\mathrm{n}}_{\mathrm{t}}) \geq 0 \\ \boldsymbol{v}^{\mathrm{n}}_{\mathrm{t}} + \left(\dfrac{L_{\mathrm{f}}}{2\,\omega_{\mathrm{b}}}\right)\left(\dfrac{\eta(\boldsymbol{x}, \boldsymbol{v}^{\mathrm{n}}_{\mathrm{t}})}{\|\boldsymbol{i}_{\mathrm{t}}\|^2}\right)\boldsymbol{i}_{\mathrm{t}} & \eta(\boldsymbol{x}, \boldsymbol{v}^{\mathrm{n}}_{\mathrm{t}}) < 0 \end{cases}$$

$$\eta(\boldsymbol{x}, \boldsymbol{v}^{\mathrm{n}}_{\mathrm{t}}) := \dot{h}\,(\boldsymbol{x}, \boldsymbol{v}_{\mathrm{t}}) + c\, h(\boldsymbol{x})$$

Without Safety Filter: DADS-BS vs PI under a 3-Phase Fault

- $v_{\mathrm{g,dq}}$ forced to 0 during $t \in [2, 4]\ s$ — worst-case grid disturbance

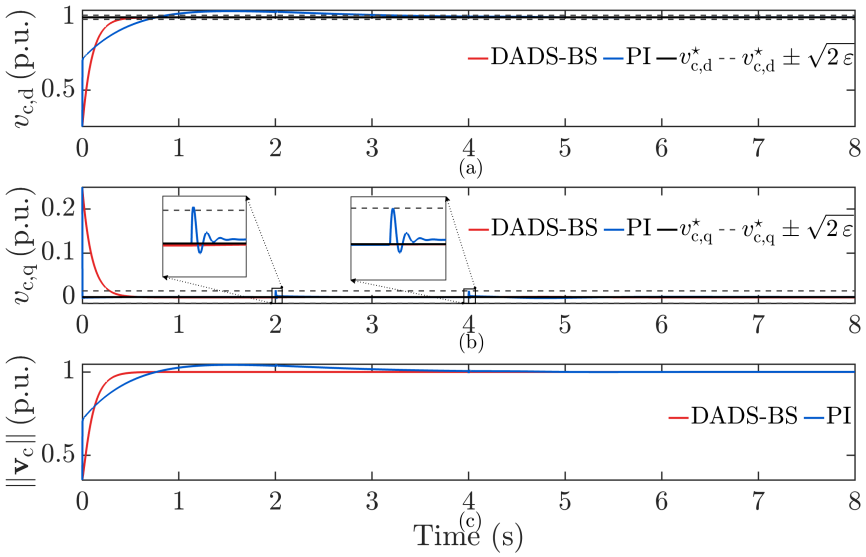

PCC voltage

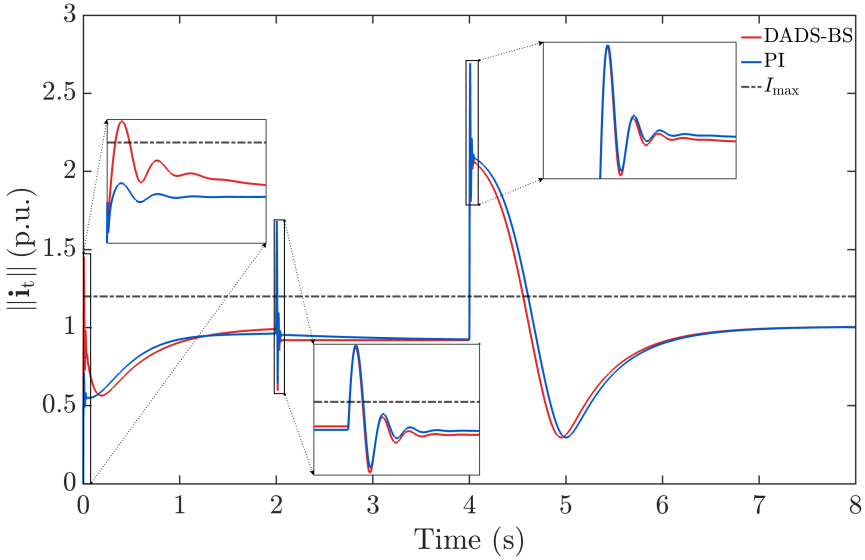

Terminal current

DADS-BS: $v_{\mathrm{c,dq}}$ stays inside the $\pm\sqrt{2\varepsilon}$ band as predicted, fault or not. **PI:** tracks nominally but residuals grow with disturbance. **Both:** $\|\boldsymbol{i}_{\mathrm{t}}\|$ blows past I_{max}= 1.2 p.u. at every transient — peaks near 2.7 p.u. at the fault transitions. This is exactly why a safety layer is non-optional.

With CBF Safety Filter: Hard Limit Holds, Recovery is Fast

- Same fault scenario; safety filter wraps each nominal controller

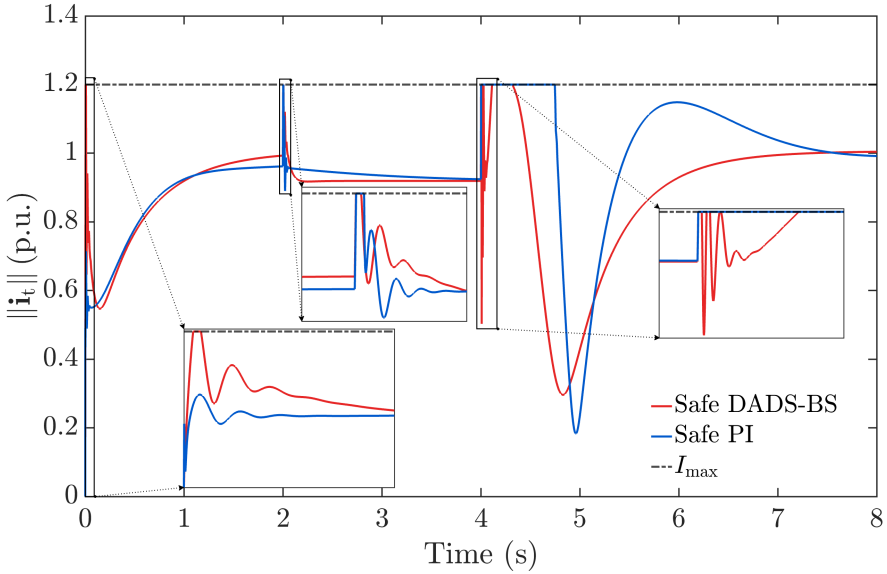

Terminal current (now bounded)

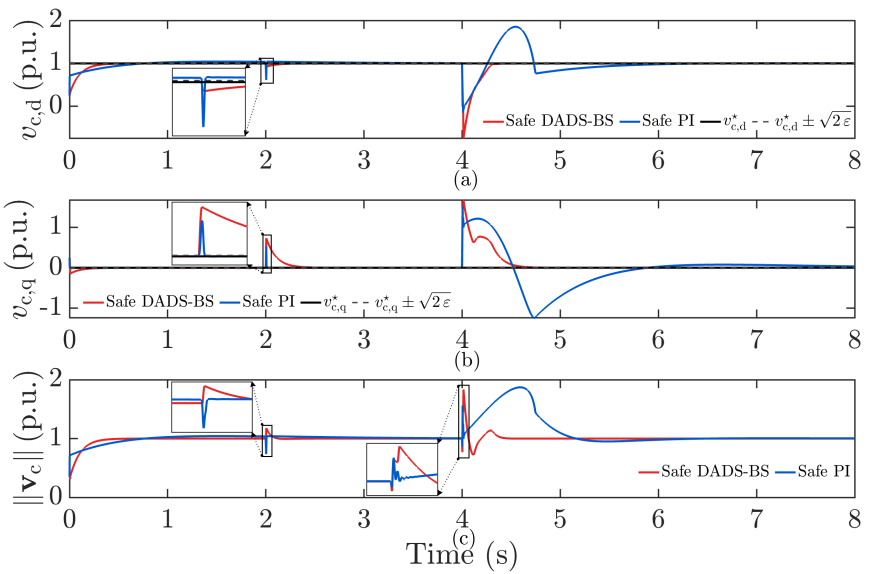

PCC voltage — temporarily relaxed

Hard limit: $\|\boldsymbol{i}_t\| \leq 1.2$ p.u. for all t — for both Safe DADS-BS and Safe PI. **Recovery:** Safe DADS-BS returns to GFM tracking faster than Safe PI after each saturation event — the adaptive damping is still doing useful work in the background while the filter is active.

Singular Solution Space Boundary

Efficient estimation of voltage collapse point via geodesic curves and limited data

Source: [1] Zheng, Qirui, Dan Wu, Franz-Erich Wolter, and Sijia Geng. "Evaluating Power Flow Manifold from Local Data around a Single Operating Point via Geodesics." arXiv preprint arXiv:2603.21514 (2026).
[2] Wu, Dan, Franz-Erich Wolter, and Sijia Geng. "Approximating voltage stability boundary under high variability of renewables using differential geometry." Electric Power Systems Research 236 (2024): 110716.

Voltage Collapse

- Iberian blackout 2025: It was voltage instability.
- The blackout was caused by an overvoltage problem with a multifactorial origin: the system had insufficient voltage control capacity, oscillations occurred that affected the operation of the system and generations were disconnected, in some cases improperly.

An interesting item in the recommendations: "…allow asynchronous installations to apply power electronics solutions to manage voltage fluctuations…".

Source: National Security Council, "The report of the April 28th electricity crisis analysis". Online access: https://www.miteco.gob.es/es/prensa/ultimas-noticias/2025/junio/se-presenta-el-informe-del-comite-de-analisis-de-la-crisis-elect.html.

Power Flow Manifold

- Power flow model: Quadratic form in voltage.

$$\mathscr{P}_i(\theta, V) = P_i^{\text{sp}} - V_i \sum_{k \in \mathcal{N}_i} V_k (G_{i,k} \cos\theta_{i,k} + B_{i,k} \sin\theta_{i,k}) = 0$$

$$\mathscr{Q}_i(\theta, V) = Q_i^{\text{sp}} - V_i \sum_{k \in \mathcal{N}_i} V_k (G_{i,k} \sin\theta_{i,k} - B_{i,k} \cos\theta_{i,k}) = 0$$

- Singular solution space boundary (SSB): The Jacobian of the power flow equation becomes singular.

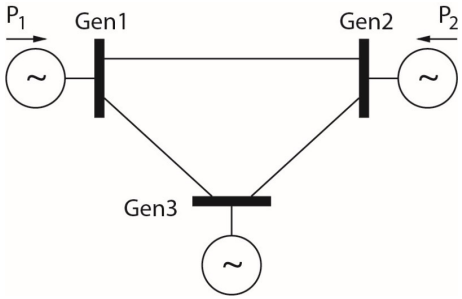

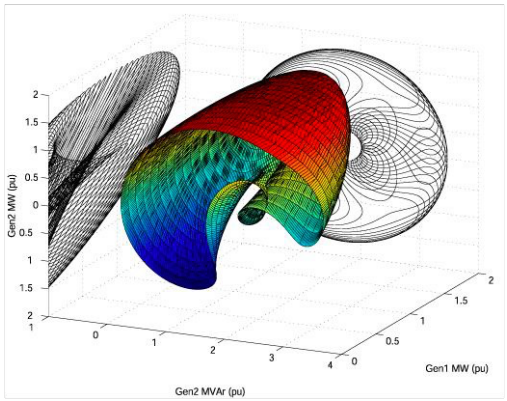

Singular Solution Space Boundary

- Power systems have finite capability to transfer power across network to supply loads. Known as the point of maximum loadability.
- Voltage collapse occurs when load-end dynamics attempt to restore power consumption beyond the capability of the system.

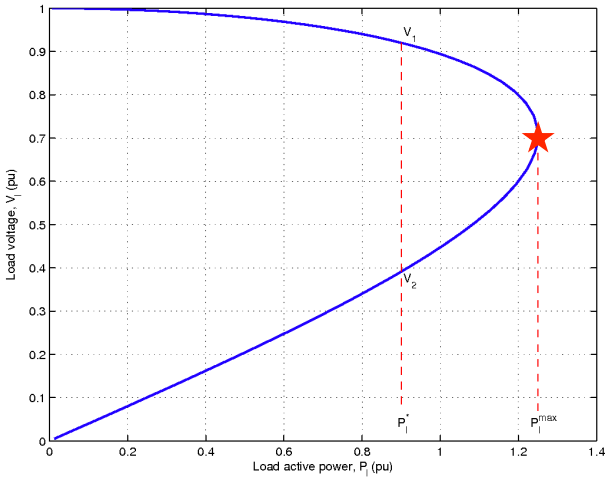

- For this example, P_l is relaxed as a variable.
- Two solutions exist for loads $P_l < {P_l}^{max}$.
- Solutions coalesce at the bifurcation point.

Singular Solution Space Boundary

- Aim: Find the SSB, which implies the stability margin at the current o.p.
- Traditional methods:
  - Continuation power flow (CPF): Specify one direction of change for load and generation pattern and seeks the trajectory of power flow along the direction of varying until reaching singularity.
  - Numerical optimization: Find the smallest voltage stability margin.

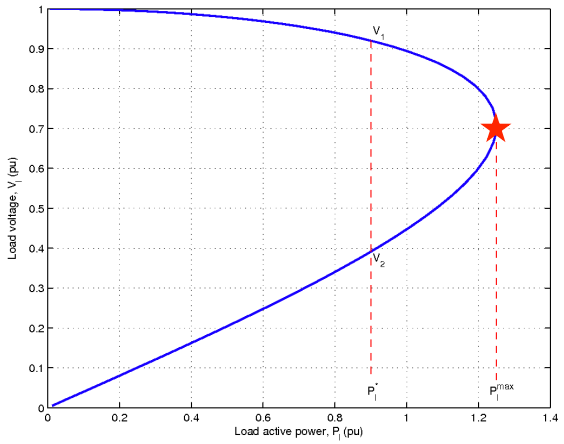

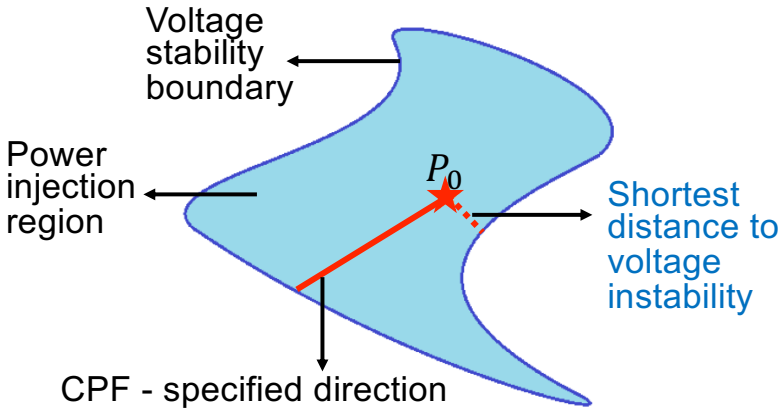

Singular Solution Space Boundary

- CPF method is computationally expensive for applications in high-dimensional systems.
- Numerical optimization is unable to reveal the global shape of the stability boundary.

Geodesic Curve

- The power flow equation is a smooth map that maps nodal voltage and angles (V, θ) to the nodal active and reactive power injections (P, Q),

$$\mathcal{F} : \mathbb{R}^N \to \mathbb{R}^N, \mathcal{F}(\mathbf{V}, \theta) = (\mathbf{P}, \mathbf{Q})$$

- For a smooth curve γ on the manifold described by $\mathbf{r}\big(\mathbf{s}(\tau)\big) : \mathbb{R} \to \mathbb{R}^{n+m}$ to be a geodesic curve, i.e., the shortest path between two points on a Riemannian manifold, γ must satisfy the geodesic equation that represents zero acceleration,

$$\frac{\partial^2 s^k}{\partial \tau^2} + \sum_{i,j}^{n} \Gamma_{ij}^k \frac{\partial s^i}{\partial \tau} \frac{\partial s^j}{\partial \tau} = 0.$$

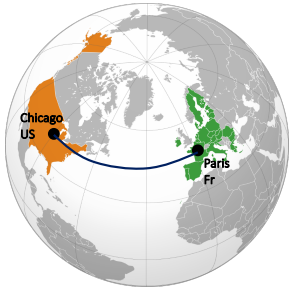

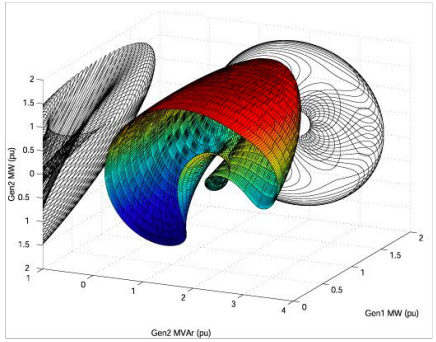

Differential Geometry Methods

- Given canonical parameterizations, we expand each voltage variable V^k at a given point $V^k(0)$ by the Taylor series:

$$V^k(\tau) \approx V^k(0) + \dot{V}^k(0)\tau + \frac{1}{2}\ddot{V}^k(0)\tau^2 .$$

- Substituting the geodesic equation: $V^k(\tau) \approx V^k(0) + \dot{V}^k(0)\tau - \frac{1}{2}\sum_{i,j}^{N} \Gamma_{ij}^k \dot{X}^i(0)\dot{X}^j(0)\tau^2 .$

- This quadratic map naturally exhibits an extremum value which provides an approximation of the voltage stability boundary.

$$\bar{V}_{appx}^k = V^k(0) + \left(\dot{V}^k(0)\right)^2 \left(2\sum_{i,j}^{N} \Gamma_{ij}^k \dot{X}^i(0)\dot{X}^j(0)\right)^{-1} .$$

Simulation Results

- A high-dimensional scenario:
  - Buses 20, 21, 22, 28 are load varying nodes with a constant power factor 0.95.
  - Buses 10, 25, 54, 100 as the renewable fluctuating nodes.

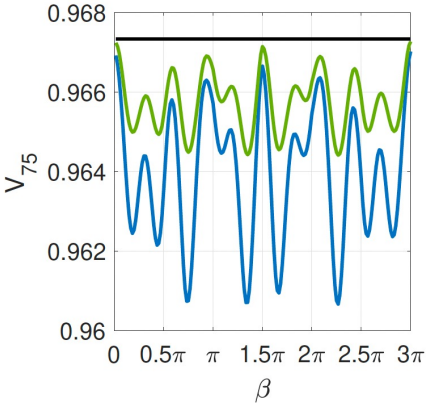

(a) V^{75} at Initial Scenario-1

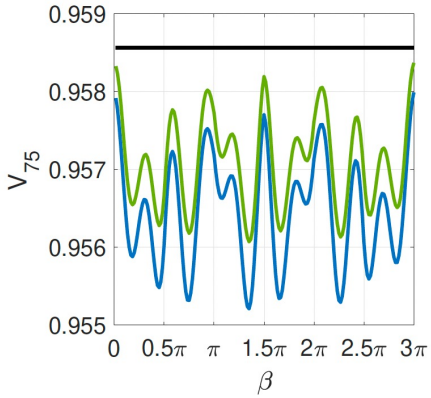

(b) V^{75} at Initial Scenario-2

Figure: Voltage stability boundary estimation for the IEEE 118-bus case.

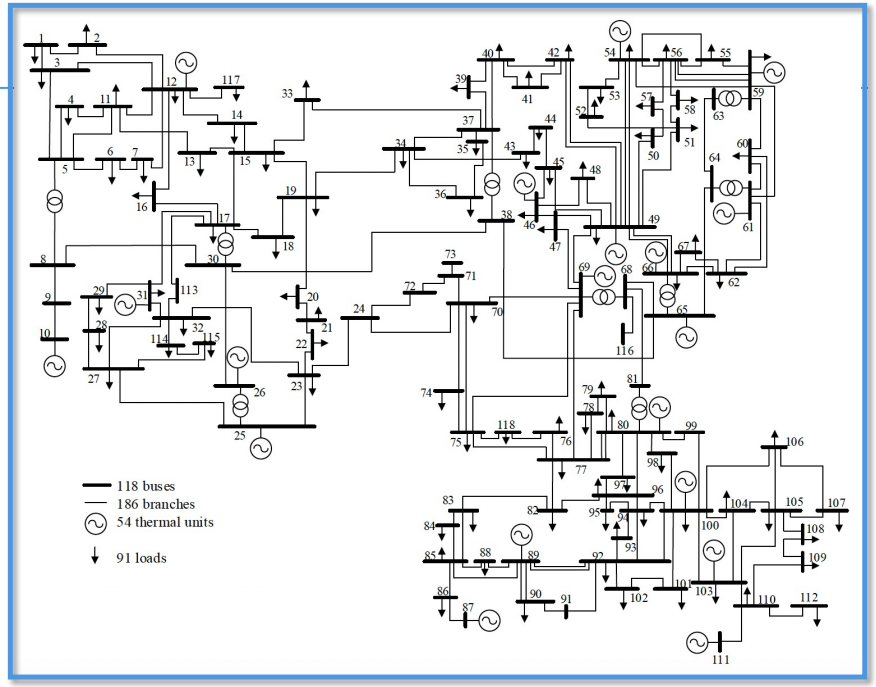

System	9-Bus	14-Bus	39-Bus
CPF [29] (sec)	10.4	17.5	42.5
CPF MATPOWER [30] (sec)	14.1	38	69.7
Christoffel computation (sec)	0.0009	0.00146	0.0136
Proposed estimation (sec)	0.0141	0.0191	0.0441
Speedup	739	916	964

Using Limited Data to Estimate Global Power Flow Manifold

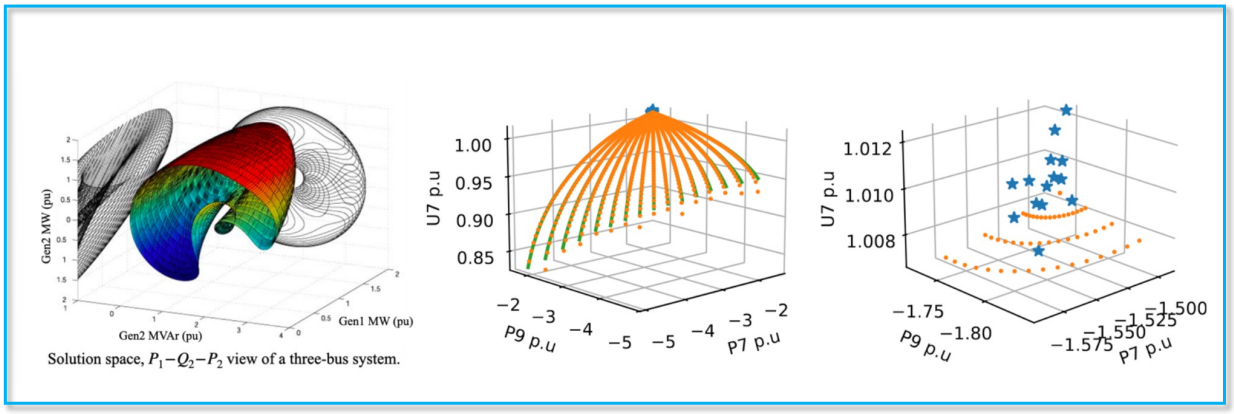

Source: Zheng, Qirui, Dan Wu, Franz-Erich Wolter, and Sijia Geng. "Evaluating Power Flow Manifold from Local Data around a Single Operating Point via Geodesics." arXiv preprint arXiv:2603.21514 (2026).

Acknowledgement

PhD Students and Postdocs at the JHU PENSA Lab

Sushobhan Chatterjee

4th-year PhD student

Shigeng Wang

2nd-year PhD student

Bhathiya Rathnayake

ROSEI Postdoctoral Fellow

Collaborators: Enrique Mallada (JHU), Richard Pates (Lund), Dan Wu (HUST), Yunjie Gu (Imperial), Tim Green (Imperial), Ian Hiskens (Umich), etc…

Thank You!

Sijia Geng, Ph.D. (sgeng@jhu.edu)
Assistant Professor
Johns Hopkins University